Nagra
Nationale
Genossenschaft
für die Lagerung
radioaktiver Abfälle

Cédra
Société coopérative
nationale
pour l'entreposage
de déchets radioactifs

Cisra
Società cooperativa
nazionale
per l'immagazzinamento
di scorie radioattive

TECHNICAL REPORT 90-12

A THERMODYNAMIC DESCRIPTION OF THE EVOLUTION OF PORE WATER CHEMISTRY AND URANIUM SPECIATION DURING THE DEGRADATION OF CEMENT

U. BERNER

MARCH 1990

Paul Scherrer Institute, Villigen

Parkstrasse 23 5401 Baden/Schweiz Telephon 056/20 55 11

Nagra
Nationale
Genossenschaft
für die Lagerung
radioaktiver Abfälle

Cédra
Société coopérative
nationale
pour l'entreposage
de déchets radioactifs

Cisra
Società cooperativa
nazionale
per l'immagazzinamento
di scorie radioattive

TECHNICAL REPORT 90-12

A THERMODYNAMIC DESCRIPTION OF THE EVOLUTION OF PORE WATER CHEMISTRY AND URANIUM SPECIATION DURING THE DEGRADATION OF CEMENT

U. BERNER

MARCH 1990

Paul Scherrer Institute, Villigen

Parkstrasse 23 5401 Baden/Schweiz Telephon 056/20 55 11

This report was prepared as an account of work sponsored by Nagra. The viewpoints presented and conclusions reached are those of the author and do not necessarily represent those of Nagra.

Preface

In the framework of its Waste Management Programme the Paul Scherrer Institute is performing work to increase the understanding of repository near field behaviour. These investigations are performed in close cooperation with, and with the financial support of NAGRA. The present report is therefore issued simultaneously as a PSI report and as a NAGRA NTB.

Zusammenfassung

In einem Endlager für "schwach– und mittelaktive" radioaktive Abfälle ist erhärterter Portlandzement als Verfestigungs-, Verfüll- und Konstruktionsmaterial von zentraler Bedeutung. Dieser Zement, in riesigen Mengen vorhanden, wird die Chemie des Endlagers über lange Zeiträume bestimmen. Mit der vorliegenden Arbeit wird versucht, das chemische Langzeitverhalten von Zement unter Endlagerbedingungen modellmässig zu erfassen, wobei insbesondere die Wechselwirkung zwischen Zement und Grundwasser im Vordergrund steht. Es wurden verschiedene Teilmodelle entwickelt, welche unter anderem die Hydratisierung von Zement, die Löslichkeitseigenschaften von Calcium–Silikat–Hydraten und die Wechselwirkung Zement – Grundwasser beschreiben. Schliesslich wird als Anwendung die Freisetzung von Uran aus einem Endlager modelliert.

Das Teilmodell zur Hydratisierung von Zement basiert auf einem Formalismus nach Bogue und auf der Annahme, dass die Vielzahl von möglichen Hydratisierungsprodukten in einige wenige charakteristische Gruppen von Modellverbindungen eingeteilt werden kann. Von allfälligen Zementadditiven (Silikatstäube, Trass usw.) wird angenommen, dass sie vollständig mit dem Bindemittel reagieren.

Das inkongruente Löslichkeitsverhalten der wichtigsten Zementphase (Calcium–Silikat–Hydrat; CSH–Gel) wird durch eine Näherung beschrieben, welche direkt in üblichen geochemischen Speziationsprogrammen verwendet werden kann. Es wird angenommen, dass CSH–Gele als eine nichtideale Mischung von unabhängigen Modellkomponenten darstellbar sind. Die Löslichkeiten dieser Modellkomponenten als Funktion der CSH–Gel–Zusammensetzung wurden aus einer Vielzahl von Literaturdaten extrahiert.

Die Resultate aus dem Hydratisierungs- und aus dem Löslichkeitsmodell wurden in einem Mischtankmodell zusammengefasst; dieses beschreibt die Auslaugung von Zement in natürlichen Grundwässern. Das Mischtankmodell geht von der Annahme aus, dass sich der Zement im thermodynamischen Gleichgewicht mit dem Grundwasser befindet. Das equilibrierte Grundwasser wird sukzessive gegen frisches Grundwasser ausgetauscht und Schritt für Schritt wird die Zusammensetzung der Zementporenlösung sowie das noch verbleibende chemische Inventar mit dem Speziationsprogramm MINEQL/PSI berechnet. Für die vollständige Degradierung einer Normmenge Zement werden ca. 5000 bis 10000 solcher Berechnungsschritte (Zyklen) benötigt. Die derart bestimmte "Lebensdauer" eines vorgegebenen Zementes hängt hauptsächlich von der Zusammensetzung des Grundwassers ab. Die Zusammensetzung von Zement hat auf die Lebensdauer nur einen sekundären Effekt, bestimmt aber das pH–Niveau der Zementporenlösung. Die Carbonat–Konzentration des Grundwassers wurde als sehr wichtiger Parameter identifiziert. Carbonat vermag gelöstes Ca^{2+} als Calzit zu fällen und beschleunigt so die Umwandlung Zement $\rightarrow$ Calzit.

Stellvertretend für die Aktiniden wurde das Löslichkeitsverhalten von Uran in der Zementporenlösung modelliert. Die Konzentration von Uran in der Porenlösung hängt weitgehend von der Wahl des löslichkeitsbestimmenden Festkörpers ab. Mit den thermodynamischen Parametern der reinen Festkörper ergeben sich Konzentrationen von ca. 10^{-4} M für U_3O_8, $USiO_4$, UO_2 und U_4O_9 und von ca. 10^{-14} M für $CaUO_4$. Die wässrige Speziation des Urans wird vom Komplex $U(OH)_5^-$ dominiert. Die kumulative Auslaugung des Urans ist ebenfalls durch die Wahl der Festphase bestimmt, Zement– und Grundwasserzusammensetzung haben praktisch keinen Einfluss. Eine realistische Menge von ca 0.1 mMol U/kg Zement ist nach 5 - 10 Zyklen im Falle von U_3O_8, nach ungefähr 100 Zyklen im Falle von UO_2, und nach 5000 - 10000 Zyklen im Falle von $CaUO_4$ als löslichkeitsbestimmende Festphase vollständig ausgelaugt.

Vorschläge zur Weiterentwicklung der Teilmodelle werden in den Schlussfolgerungen dargelegt.

Abstract

Portland cement, used as solidification–, backfill– and construction–material, is considered to determine the chemical behaviour of a low– and intermediate level radioactive waste repository for very long periods of time. In order to describe the long term chemical behaviour of such cement based structures, a series of submodels including the hydration of cement, the thermodynamic properties of calcium–silicate–hydrates and the degradation of hydrated cements in natural groundwaters have been developed. As an application, the leaching of uranium from a cement based structure is modelled.

Cement hydration is modelled using Bogue's method. The variety of possible hydrated cement minerals is classified into several groups of model solids. Cement additives (e.g. silica fume, trass etc.) are assumed to react completely with the cement.

The incongruent solubility behaviour of calcium–silicate–hydrates (CSH–gels) is described using an approach directly applicable to common geochemical speciation codes. Based on the assumption that CSH–gels may be described by independent model components, their solubility properties are extracted from a large amount of literature data. Solubility constants are given as a function of the CSH–gel composition.

Within a mixing tank model, the results of the hydration and of the solubility model are used to describe the degradation of cement in natural groundwaters. The mixing tank model assumes thermodynamic equilibrium between hydrated cement and groundwater and recalculates the speciation of solutes in the pore solution and the remaining chemical inventory in consecutive steps (cycles). It takes some 5000 to 10000 cycles to completely degrade the hydrated cement. The particular "lifetime" depends mainly on the groundwater composition. The composition of the cement has a secondary effect on lifetime, but it determines the absolute pH level and the relative time period of high pH conditions ($pH \geq 12$) in the pore solution. Carbonate concentration in the groundwater is found to be a very important parameter, due to transformation of hydrated cement minerals into calcite.

As a representative for the actinides, the solubility behaviour of uranium in degrading cement is modelled assuming an Eh of -300 mV. The uranium concentration in the pore solution is determined by the "choice" of the solubility limiting phase. If the speciation is calculated by using the thermodynamic solubilities of the pure solids, concentration levels of about 10^{-4} M are found for U_3O_8, $USiO_4$, UO_2, U_4O_9 and of 10^{-14} M for $CaUO_4$. Cumulative uranium leaching from hydrated cement is found to be nearly independent of cement and groundwater composition, but strongly dependent on the properties of the solubility limiting phase. An amount of 0.1 mmoles U/kg hydrated cement is completely leached out after 5 to 10 cycles using U_3O_8 as the solubility limiting solid, after $\sim$100 cycles using UO_2 and after $\sim$5000 (to 10000) cycles using $CaUO_4$.

Recommendations for further development of the submodels and appropriate priorities are given in the conclusions.

Résumé

L'influence du ciment Portland, utilisé comme matériau de solidification, de colmatage ou de construction, sur le compartment chimique à long terme d'un dépôt final pour déchets de faible et de moyenne activité a été étudié. Afin de décrire le compartement chimique à long terme d'éléments à base de ciment, une série de sous–modèles ont été développé, relatifs à l'hydratation du ciment, aux propriétés thermodynamiques d'hydrates de silicates de calcium et à la dégradation de ciments hydratés par des eaux souterraines naturelles. La lixiviation d'uranium à partir d'une matrice de ciment a été modélisée à titre d'application.

L'hydradation du ciment est modélisée en utilisant la méthode de Bogue. Les diverses variétés de minéraux de ciments hydratés possible sont classées en plusiers groupes de solides modèles. On part de l'hypothèse que les additifs au ciment (par ex. silica fume, trass) réagissent totalement avec celui–ci.

Le compartement de la dissolution incongruent des hydrates de silicates de calcium (gels (CSH) est décrit en utilisant une approache directement applicable aux codes des spéciations géochimiques communes. Se fondant sur l'hypothèse que les gels CSH peuvent être décrits par des composantes indépendantes de modèles, leurs propriétés de solubilité sont tirées d'une grande quantité de données trouvées dans la littérature. Les constantes de solubilité sont donées en fonction de la composition de gels CSH.

Les résultats de modèles d'hydratation et de dissolution sont utilisés pour décrire la dégradation du ciment par des eaux souterraines naturelles en partant d'un modèle à récipient mélangeur. Le modèle à récipient mélangeur présuppose un équilibre thermodynamique entre le ciment hydraté et l'eau souterraine et recalcule la spéciation des solutés dans les solutions à l'intérieur des pores ainsi que l'inventaire chimique restant, par étapes successives (cycles). Il faut compter circa 5000 à 10000 cycles pour dégrader totalement un ciment hydraté. La "durée de vie" en question dépend essentiellement de la composition de l'eau souterraine. La composition du ciment n'a qu'une influence secondaire sur la durée de vie mais elle détermine le niveau du pH absolu et la période relative durant laquelle les conditions de pH élevé (pH $\geq$ 12) sont maintenues dans la solution à l'intérieur des pores. La concentration de carbonates dans l'eau souterraine s'avère être un paramètre très important en raison de la transformation des minéraux de ciments hydratés en calcite.

La dissolution de l'uranium dans un ciment en cours de dégradation est modélisée, à titre représentatif pour les actinides, en supposant un Eh de -300 mV. La concentration d'uranium dans la solution des pores est déterminée par le "choix" de la phase limitant la solubilité. Si la spéciation est calculée en utilisant les solubilités thermodynamique des pure solides, des niveaux de concentration de l'ordre de 10^{-4} M sont trouvés pour U_3O_8, $USiO_4$, UO_2, U_4O_9 et de 10^{-14} M pour $CaUO_4$. On trouve q'une lixiviation cumulative d'uranium à partir de ciments hydratés est presque indépendante de la composition du ciment et de celle de l'eau, mais qu'elle dépend fortement des propriétés de la phase limitant la solubilité. Une quantité de 0.1 mmole U/kg de ciment hydraté est complètement lixiviée après 5 à 10 cycles si l'on utilise U_3O_8 comme solide limitant la solubilité, après $\sim$ 100 cycles avec UO_2 et après $\sim$ 5000 (jusqu'à 10000) cycles avec $CaUO_4$.

Ce rapport se termine par des recommandations pour le développement ultérieur de sous–modèles et conclut par une liste de priorités appropriées.

Contents

List of Figures

List of Tables

1 Introduction

In Switzerland disposal of radioactive wastes into geological formations is foreseen, but a repository will be built only if a safety analysis has demonstrated that any radionuclides which may escape from the repository remain well below authorised levels. Preliminary safety analyses have been performed in 1985 [1]. At present the corresponding models are revised and developed further and work on the required basic data is being performed.
This report is concerned with the near field modelling of a low– and intermediate level radioactive waste repository. In contrast to the high level repository which includes waste glasses, steel and bentonite, the intermediate level repository will incorporate reinforced concrete and will include large amounts of cemented waste matrices (additional waste forms e.g. bitumen or polystyrene not being considered in this report). Huge amounts of hydrated cement (several hundred thousand tons) will therefore determine the chemical and physical properties of the repository near field. For this reason, attempts have been made to model the long term evolution of cementitious material under repository conditions. Investigations on cemented waste leaching and on transport properties of radionuclides in cement are complementary research topics.
Cement reacts with water to form very stable hydrates which will control the chemical environment for a very long period of time. In a first part of the present study the hydration of cement is modelled, based on the chemical inventory of the cement and on the knowledge of the hydrates formed during hydration of the cement. The resulting set of model solids then serves as the input for modelling the degradation of the hydrated cement.
Hydrated cement phases will be converted and degraded by the groundwater infiltrating the repository. The complex and incongruent solubility behaviour of the most relevant hydrated cement phases (calcium–silicates–hydrates; CSH–gels) is the subject of a second part of the report. With these two models, the prerequisites for the description of the long term behaviour are given.
A simple mixing tank model, applied to a mixture of hydrated cement and groundwater, is then used to simulate roughly the temporal chemical evolution of the cement.
Examples of realistic cements and groundwaters are used to predict the course of development of important chemical parameters, such as pH and concentrations of relevant solutes. The parameters determining the lifetime of the chemical inventory are identified and their influence on lifetime is estimated quantitatively.
Finally, a last part is concerned with the solubility behaviour of uranium in degrading cement. The selected example shows how the release of radionuclides from a repository can be modelled, and which parameters are essential for describing the release of radionuclides. Uranium is taken here as being representative of the actinides for several reasons. Many complexes and solids of uranium and their thermodynamic properties are fairly good known and in addition uranium may be present in different oxidation states, which enables to study the influence of varying redox conditions.

The validity of the applied thermodynamic approach is discussed and basic features for further model development are identified.

The main emphasis of the present study is on

- the identification of relevant mechanisms and parameters
- the development of quantitative models
- the presentation of quantitative results obtained by the models using realistic examples

Main emphasis is also placed on the integration of the different submodels and on their impact on the final results. As a first step it was deliberately decided not to develop individual model parts in great detail. The examples selected essentially serve for the identification of parameters relevant to the systems considered and for illustration of the problems which have to be examined with first priority in further detailing of the models. This seems to be a necessary procedure, since it is obvious that not *all* open questions may be answered in a satisfactorily manner within the available period of time. On the other side, the questions relevant to safety analyses *must be answered* and should therefore be identified as soon as possible and assigned *high priority*.

2 Hydration of portland cement

Hydrated cement minerals form the basic substances for modelling of the degradation of cement based barrier and matrix materials (including subsequent modelling of cement pore water and radionuclide speciation). In principle, these hydrated cement minerals could be identified qualitatively or quantitatively by experiment, but such experiments are very expensive and could be carried out (if at all practical) only for selected, very specific cement systems. In addition, the gain from such a detailed analysis would be questionable since hydrated cements contain a variety of minor components (typically less than 1 % by weight) which may exhibit similar structural and thermodynamic properties. The bulk chemistry of hydrated cement is largely defined by a system containing CaO, Al_2O_3, Fe_2O_3, SiO_2, SO_3 and H_2O and attempts have been made to model the most important hydration processes of portland cement using some simplifying assumptions [2,3,4].

Table 1: Model solids proposed in the cement hydration model [2,3]. For comparison the model solids from Glasser's model [4] are also given.

This study	Model of Glasser
C_3AH_6—C_3FH_6 (solid solution)	
$C_3A.3C\bar{S}.32H$ (Ettringite)	
$C_3A.C\bar{S}.12H$ (low-sulphate)	$C_4(A,F).13(H,\bar{S})$ (AF_m–type phases)
	C_2ASH_8 (Gehlenite hydrate)
C_xSH_x ($x \leq 1.8$)	C_xSH_y ($0.9 \leq x \leq 1.8$; y:saturation assumed)
CH ($Ca(OH)_2$; Portlandite)	CH
MH ($Mg(OH)_2$; Brucite)	$M_{5.3}AH_y$ (Hydrotalcite; y:saturation assumed)

Nomenclature: C = CaO, S = SiO_2, A = Al_2O_3, F = Fe_2O_3, H = H_2O, $\bar{S}$ = SO_3, M = MgO

Our recently published model [2,3] starts from the calculation of the clinker[1] phases assembly, according to the method of Bogue [5]. The model is capable of considering the hydration reactions of each clinker mineral individually and independently by setting the appropriate parameters, but the variety of possible reaction products is condensed into a few characteristic groups of model solids. For blended cements it is assumed that the blending agent (i.e. slag, trass, silica fume etc.) reacts completely with the portland cement and that no new phases are generated. A more detailed description and also some numerical results of the hydration model are given in [2,3].

The model of Glasser [4] is based on the application of the phase rule. As in our model the variety of possible hydrated minerals is condensed into characteristic groups of model solids (each group is represented by a single, well defined solid). In contrast to our model, the range of hydrated cement compositions is divided into contiguous phase regions. The phase assemblages within each region satisfy the phase rule and have been confirmed experimentally. Glasser also assumes a complete reaction of added blending agents with the cement. A comparison of the resulting model solids is given in Table 1.

Within these models the assumption of complete reaction of a blending agent with the cement is hard to prove experimentally (an exception is pointed out in [6], for a cement blended with reactive silica fume). After a period of high reactivity (1 - 3 months), many phase conversion reactions will continue very slowly (years or tens of years; cf. also [7,8]) and it is not sure whether the on-going reactions will reach completion or whether the system will reach a thermodynamically stable state. This questions as to the final thermodynamic state of a cement system is still open and it is quite likely that the degradation of cements in a repository environment starts (due to leaching processes) before the system has reached a stable (or a persistent meta–stable) state. Therefore, the assumption of a final thermodynamic state and of the completeness of reactions with blending agents is essential in the sense that it enables the modeller to break the whole model chain into separated submodels and to exclude kinetic considerations in a first approach.

[1] unhydrated, not yet milled cement is called *clinker*

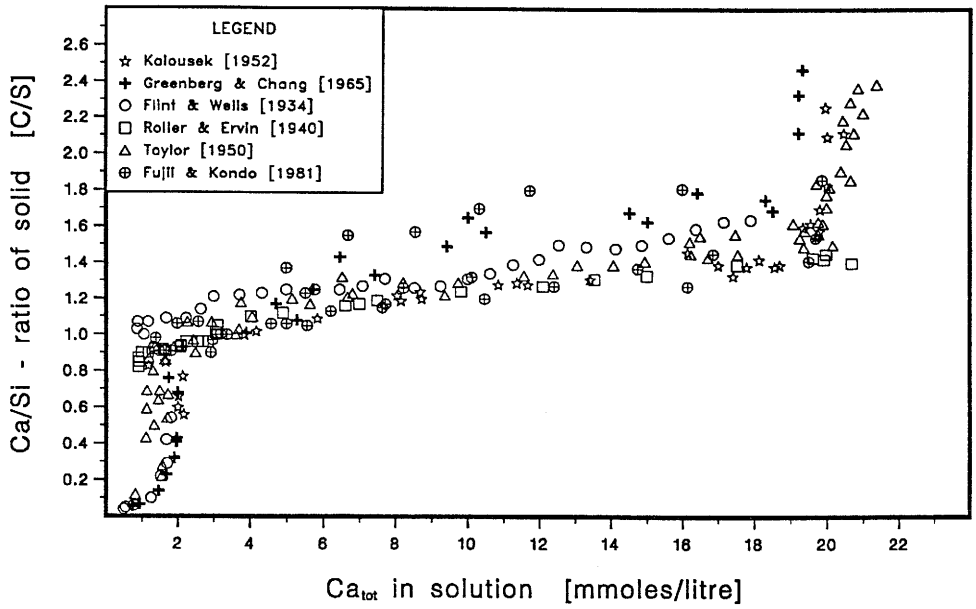

Figure 1: Measured Calcium Concentrations in the System $CaO–SiO_2–H_2O$

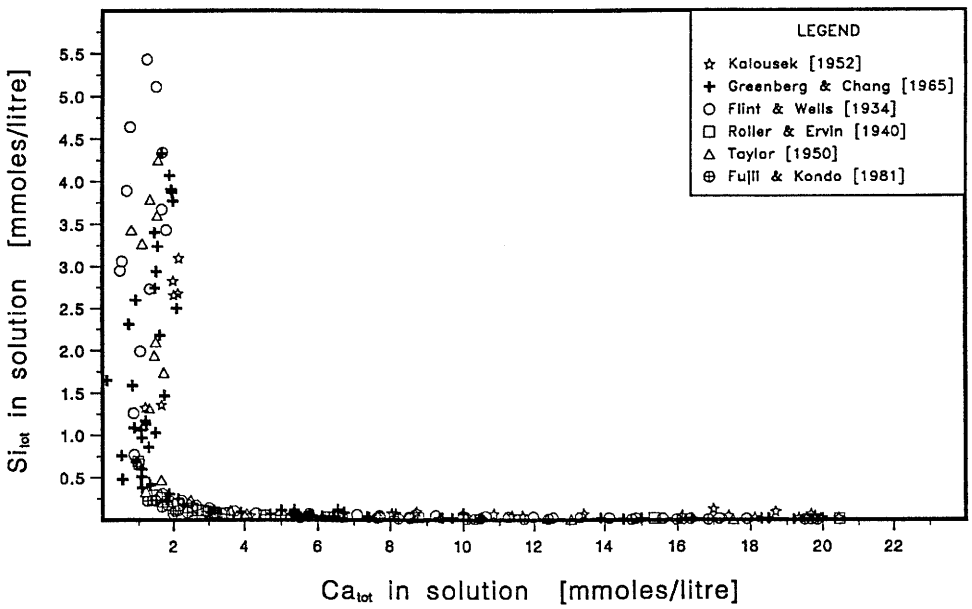

Figure 2: Measured Silica Concentrations in the System $CaO–SiO_2–H_2O$

3 The solubility model for CSH–phases

The most important solid phase within a hardened cement is the CSH–gel (Calcium Silicate Hydrate). A general composition of $xCaO.SiO_2.yH_2O$ is assumed for these phases, where x lies in the range 1.4 to 1.8 for common portland cements and $y \geq x$ (for silicon-rich cement blends x may decrease to values near 1). The experimental data [9,10,11,12,13,14] (cf. Figures 1 and 2) clearly show the incongruent dissolution behaviour of the CSH–phases. In general a dissolution according to

$$xCaO.SiO_2.yH_2O_{(s)} \rightleftharpoons p \cdot Ca(OH)_{2\ (aq)} + q \cdot SiO_{2\ (aq)} \qquad (1)$$

with $\frac{p}{q} \neq x$ is observed. Up to now it is not clear whether reaction 1 is a true thermodynamic equilibrium or not, but the assumption of a meta–stable persistent equilibrium (compared to laboratory time scales) seems to be fulfilled. For x–values above 1, the ratio p/q is generally large (> 1000), which means, that CSH–phases with C/S > 1 mainly produce dissolved $Ca(OH)_2$ and only traces of dissolved SiO_2 . Congruent solubility (p/q = x) of CSH–phases is observed at C/S–values below 1 but the actual value strongly depends on the composition of the solution (for pure water, congruent solubility is observed at x $\sim$ 0.8, which is the C/S ratio of natural Tobermorite).
The values for p and q are not known a priori, but have to be determined experimentally for each particular C/S ratio. Due to this fact, the thermodynamic modelling of CSH–phases using common geochemical speciation codes becomes complicated in the sense that for each particular C/S ratio a specific dissolution reaction (given by p,q and $\log K_{so}$) has to be defined. Unfortunately common speciation codes are not set up for handling equations with variable, non-integer stoichiometric coefficients and with composition dependent equilibrium "constants".

Within these geochemical speciation codes (MINEQL, PHREEQE, EQ3/6) the solubility of solids is described using a dissociation process with stoichiometric coefficients given by the solids :

$$A_aB_{b\ (s)} \rightleftharpoons a \cdot A_{(aq)} + b \cdot B_{(aq)}. \qquad (2)$$

It is obvious that at least 2 independent equations of type 2 are required to model an equation of type 1.
The main aim of the solubility model for CSH–phases is to describe type 1 equilibria by using equations of type 2. This will enable the use of common speciation codes for modelling the dissolution behaviour of CSH–phases without further development of these codes.
As mentioned before, at least two independent type 2 equations are required to model a type 1 process. The model therefore assumes that the CSH–phases may be described using a non-ideal mixture of two components, each of them being treated as a single solid phase. With this assumption the problem of "unknown", non-integer stoichiometric coefficients (cf. p and q in equation 1) and a composition dependent equilibrium "constant" of a single phase (CSH) has been transformed into a problem of two solid components with "unknown" solubilities but with constant and fixed stoichiometric coefficients (see also [15] for a comprehensive description of the dissolution model for CSH–phases). The measured solubility data of the CSH–H_2O–system (Figures 1,2) clearly indicate three regions of different solubility behaviour (a schematic representation is shown in Figure 3, page 7). Similar regions have already been proposed by Glasser [6, Figure 9] and by Greenberg [11]:

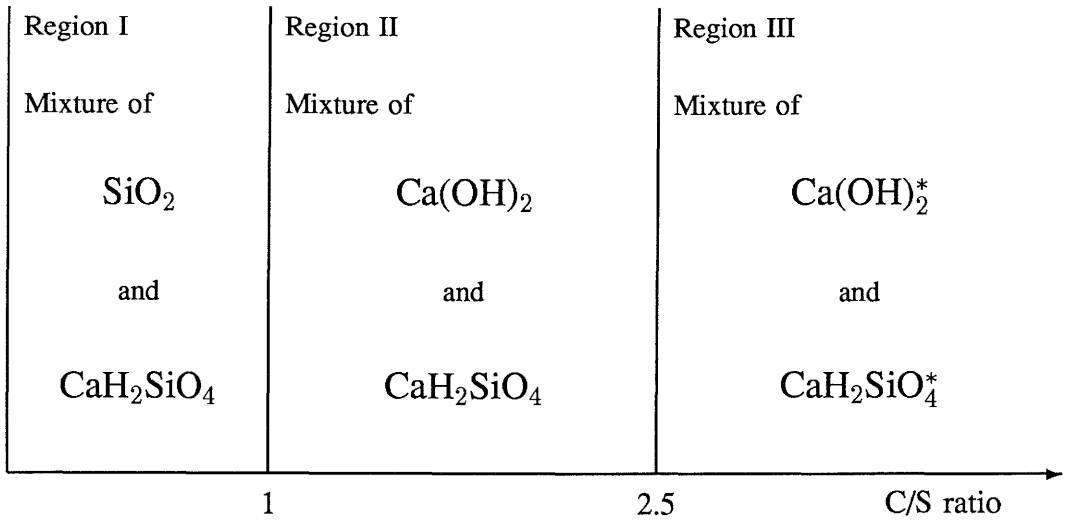

Figure 3: Schematic representation of the different C/S regions assumed in the model and of the model solids comprising the CSH–gel within each region. The solubilities of the model solids within region I and II are assumed to be C/S–dependent, whereas the solubilities of the model solids within region III (marked with a *) are assumed to be constant.

Region I:
At C/S < 1 the concentration of calcium does not exceed a value of ~ 2 mmoles/litre (Figure 1), whereas the silica concentration passes through a maximum of ~ 5 mmoles/litre (Figure 2). This means that comparable amounts of calcium and silica contribute to the composition of the equilibrium solution. A mixture of the model components SiO_2 and CaH_2SiO_4 according to Greenberg [11] is therefore assumed to describe the solid and the equilibrium situation.

Region II:
Within this region the composition of the solution is dominated by calcium hydroxide which changes from ~ 2 to ~ 21 mmoles/litre. Silica remains at a low level of 0.1 to 0.01 mmoles/litre. A mixture of the model components $Ca(OH)_2$ and CaH_2SiO_4 is therefore chosen to describe the solid.

Region III:
Calcium and silica vary just slightly with increasing C/S ratio. Calcium remains more or less constant at the level of portlandite ($Ca(OH)_2$) saturation ($\sim$ 21 mmoles/litre) and the silica concentration is as low as in region II ($\sim$ 0.01 mmoles/litre). An obvious change in silica concentrations is not observed. It is therefore assumed that calcium and hydroxide concentrations in solution are best described by using portlandite (exhibiting a constant, well defined solubility product) as the first model component. CaH_2SiO_4 with a constant solubility product is chosen as the second model component. Region III differs from regions I and II by the fact that not a non-ideal mixture of two components but two completely independent solids are used to model

the behaviour of the CSH–phase. The results will show that this assumption is justified.

It is not clear, at which C/S ratio region III is to be started. From Figure 1 a value of approximately 1.8 can be extracted, which is also found to be the maximum ratio for the CSH–phase in hydrated and aged portland cements. Locher [16] suggested that the lime-rich hydrated calcium silicates consist of tobermorite–like layers with associated calcium hydroxide layers. From this work, a lower limit of C/S $\sim$ 2.7 for region III could be concluded.
During the hydration of a portland cement, a fair amount of pure portlandite ($Ca(OH)_2$) is produced contemporary with the CSH–phases and a global "C/S" ratio (which does not distinguish between CSH and portlandite) of 2.7 or even more may result. In order to simplify the modelling, a value of C/S = 2.5 as the starting point of region III is chosen for this study. Using this value, all available experimental data lie within region I or II.

The basic thermodynamic considerations and also the procedures of extracting the actual type 2 equations from literature data are described in **Appendix A** and the corresponding literature data are compiled in **Appendix B**.
Two slightly different sets of basic thermodynamic data have been used to extract the model equations from the data. These two sets are given in Table 2 (page 9).

3.1 Results

As schematically represented in Figure 3, the phase CSH consists of two independent model solids. These model solids may be different for different C/S–regions. The basic results given within this section are the thermodynamic properties of the model components as a function of the C/S ratio. The actual dependencies are given in Table 3 (page 10). As an example, equations 3 and 4 show, how the solubility of a CSH–gel with C/S = 1.2 is modelled using the dependencies given in Table 3 (dataset 1):

$$Ca(OH)_{2(s)} \rightleftharpoons Ca^{2+} + 2 \cdot OH^-; \qquad \log \hat{K}_{so} = -5.91 \tag{3}$$

$$CaH_2SiO_{4(s)} \rightleftharpoons Ca^{2+} + H_2SiO_4^{2-}; \qquad \log \hat{K}_{so} = -8.16. \tag{4}$$

It has to be noted, however, that both equilibria have to be considered simultaneously.
Using the values given in Table 2 (basic thermodynamic data) and those given in Table 3, the solubility of CSH–phases in pure water has been modelled over the whole range of "possible" C/S ratios. The results are given in Figures 4 to 6 (page 11 and 12).

Table 2: Basic thermodynamic data used to extract model equations from literature data

Chemical Equilibrium	dataset 1†		dataset 2‡	
	logK	ΔH^{0} [1)] (kJ/mole)	logK	ΔH^{0} [1)] (kJ/mole)
$Ca^{2+} + OH^{-} \rightleftharpoons CaOH^{+}$	1.3	8.20	1.4	5.02
$H_2SiO_4^{2-} + H^{+} \rightleftharpoons H_3SiO_4^{-}$	13.1	-41.8	11.69	-87.1
$H_3SiO_4^{-} + H^{+} \rightleftharpoons H_4SiO_4^{0}$	9.86	-20.9	9.93	-37.2
$OH^{-} + H^{+} \rightleftharpoons H_2O$	14.00	-55.8	14.00	-55.8
$SiO_{2(s)} + 2{\cdot}H_2O \rightleftharpoons H_4SiO_4^{0}$	-2.70	18.4	-2.71	9.2
$Ca(OH)_{2(s)} \rightleftharpoons Ca^{2+} + 2{\cdot}OH^{-}$	-5.15	-18.1	-5.15	-16.0
$CaH_2SiO_{4(s)} \rightleftharpoons Ca^{2+} + H_2SiO_4^{2-}$	-8.16[2)]	$\sim$ -54[2)]	-7.12[3)]	$\sim$ -12[3)]

† Basic data from MINEQL/PSI (T = 25 °C)

‡ Basic data from PHREEQE (T = 25 °C)

1) Not all experiments have been performed at 25°C. A possible method for temperature correction of experimental data is given in appendix A.3.

2) Values are valid in conjunction with dataset 1 only

3) Values are valid in conjunction with dataset 2 only

3.2 Discussion

The results show that the model correctly predicts the composition of the equilibrium solutions. This is not very surprising since the model parameters have been extracted from these solution data. It is therefore important to note that the model only describes the dissolution behaviour of the solid and not the solid itself. Evidence for a "homogeneous" mixture of distinguishable components as assumed in the model is not found in reality. Hydrated calcium silicates have a layered structure over a broad C/S range ($0.7 < C/S < 1.5$). For this reason the application of the model is restricted to the field of data shown in Figures 4 to 6. For example, it would be wrong to conclude the existence of a pure solid like CaH_2SiO_4 from the model, since particular structural aspects of the hydrated calcium silicates are not included within the basic model assumptions.

Table 3: The simplified chemical system used to model the incongruent dissolution of hydrated calcium silicates (T = 25 °C). For a more detailed derivation of the actual values see Appendix A.

Region	C/S range	Model components	Data set	Apparent solubility product of model components as a function of C/S
	C/S = 0	SiO_2	1	$\log \hat{K}_{so} = -2.70$
			2	$\log \hat{K}_{so} = -2.71$
I	$0 < C/S \leq 1$	SiO_2	1	$\log \hat{K}_{so} = -2.04 + \frac{0.792}{C/S-1.2}$
			2	$\log \hat{K}_{so} = -1.994 + \frac{0.861}{C/S-1.2}$
		CaH_2SiO_4	1	$\log \hat{K}_{so} = -8.16 - \frac{1-C/S}{C/S} \cdot (0.78 + \frac{0.792}{C/S-1.2})$
			2	$\log \hat{K}_{so} = -7.12 - \frac{1-C/S}{C/S} \cdot (0.79 + \frac{0.816}{C/S-1.2})$
II	$1 < C/S \leq 2.5$	$Ca(OH)_2$	1	$\log \hat{K}_{so} = -4.945 - \frac{0.338}{C/S-0.85}$
			2	$\log \hat{K}_{so} = -4.945 - \frac{0.338}{C/S-0.85}$
		CaH_2SiO_4	1	$\log \hat{K}_{so} = -8.16$
			2	$\log \hat{K}_{so} = -7.12$
III	$C/S > 2.5$	$Ca(OH)_2$	1	$\log \hat{K}_{so} = -5.15$
			2	$\log \hat{K}_{so} = -5.15$
		CaH_2SiO_4	1	$\log \hat{K}_{so} = -8.16$
			2	$\log \hat{K}_{so} = -7.12$

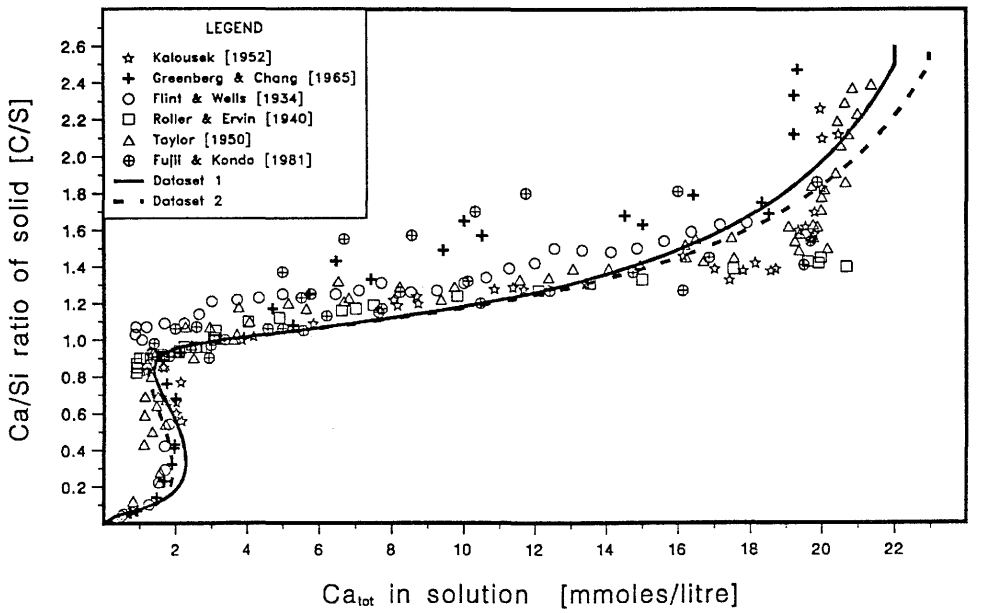

Figure 4: Model calculation of calcium concentrations in the system $CaO–SiO_2–H_2O$ using the data given in Tables 2 and 3 (T = 25 °C).

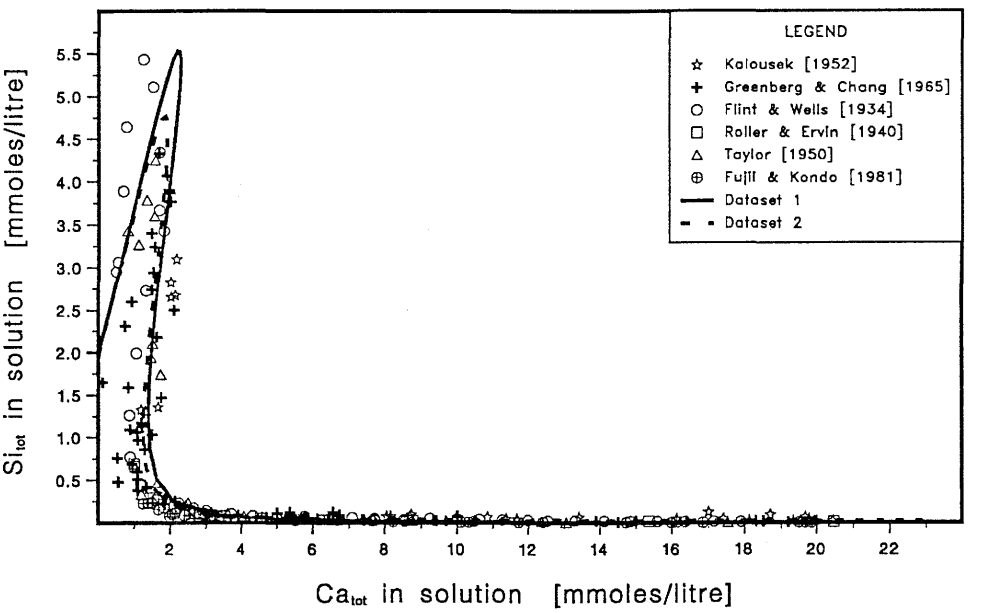

Figure 5: Model calculation of silica concentrations in the system $CaO–SiO_2–H_2O$ using the data given in Tables 2 and 3 (T = 25 °C).

Equilibrium: A basic assumption of the model is the existence of a true thermodynamic equilibrium. This assumptions seems to be correct within the short time scale of the experimental set-up (5 days up to 6 month to reach equilibrium) and was checked by the different authors. However, some of the data indicate a certain alteration of the hydrated calcium silicates with time and temperature. Using an altered calcium silicate (50°C, 1–3 month) Greenberg [11] and Fujii [10] found lower equilibrium concentrations than in unaltered calcium silicates at a constant C/S ratio, which means that the solid had become more stable due to alteration.

It is therefore reasonable to assume that the hydrated calcium silicates will reach a thermodynamically more stable state at larger time scales as proposed by this model. If this assumption holds, the model predicts the dissolution behaviour in a conservative sense (the real solubilities will be lower than the predicted one's).

Temperature: In a strict sense the model calculations are valid only at 25°C due to lack of corresponding thermodynamic data. With a procedure proposed in appendix A.3, the model may probably be used within a somewhat expanded temperature range of about 15°C to 35°C. In order to use the model at elevated temperatures (50–60°C) the need of further experimental data is indicated.

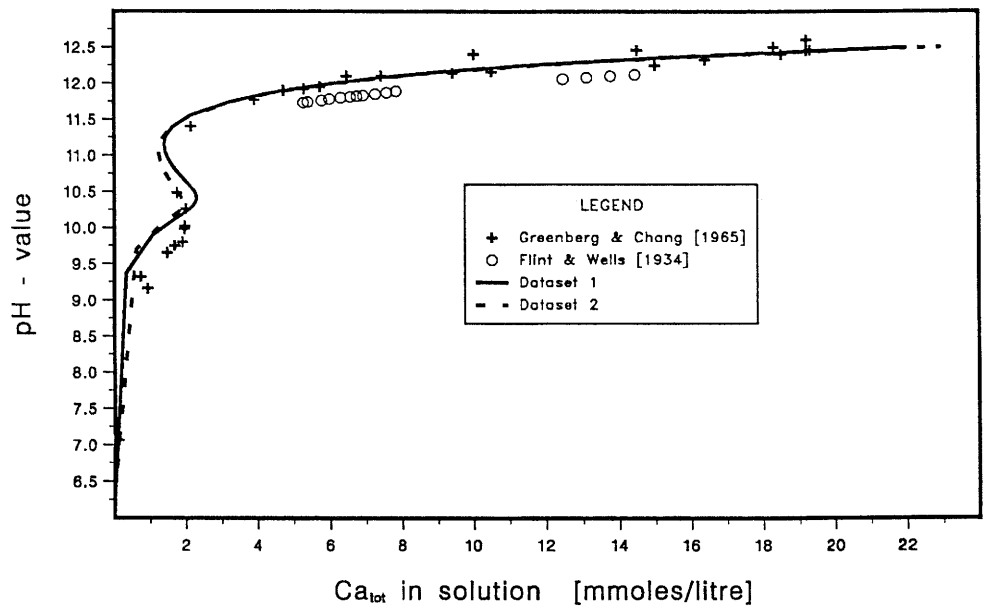

Figure 6: Model calculation of pH in the system $CaO–SiO_2–H_2O$ using the data given in Tables 2 and 3 (T = 25 °C).

4 Model solids and solutions used in the present study

4.1 Binding materials (cements)

In Switzerland a French sulphate resistant cement (HTS; Ciment Portland Artificiel, CPA 55 Haute Teneur en Silice, Ciments Lafarge, France) mixed with a German Trass (Rheinischer Trass) is widely used for the solidification of ion exchange resins from power plants [17]. A Swiss sulfate resistant portland cement (Sulfacem, Olten) is a possible candidate for constructing-, lining- and backfill materials. Therefore, these cements have been chosen for model materials within the present study. In particular a mixture of 100 parts of HTS–cement, 30 parts of trass and 52 parts of water was considered to be the basic binding material for the solidification of ion exchangers. These mixing ratios lead to a water to cement+trass ratio of 0.43. A water/cement ratio (W/C) of 0.43 was also used to model the hydration of the sulphate resistant cement. The chemical composition of the raw materials is compiled in Table 4.
The compositions given in Table 4 have to be regarded as averaged values. In reality the composition may vary slightly from batch to batch. The composition of the Sulfacem cement was provided by the producing factory. Two different samples of the HTS–cement were analysed by two different laboratories, the results showed slight differences between the two batches and between the two laboratories. The average composition provided by the factory was taken for this study. The composition of the trass was taken from Ludwig and Schwiete [18], the chemical analysis of the actual material showed a fairly good agreement with the values provided by [18].
The hydrated cement composition was calculated according to the model mentioned above [2,3], the appropriate values are given in Table 5 as mmoles / kg of hydrated cement. For comparison, the hydration products of the blended cement were also calculated using Glasser's [4] hydration model.
As expected, the two models differ in the chemical composition of the calcium-aluminate-ferrite-phase and of the Mg bearing phases. There is only a small difference in the quality of the resulting CSH–phase. However, in this first approach of modelling the degradation of cement the aluminate-, ferrite- and sulphate containing phases are not considered and, with regard to the remaining phases, the two models do not differ significantly.

4.2 Model solutions

Two different solutions have been used to model the degradation of the binding materials described in section 4.1. Pure water as one degrading solution serves as a standard and the results using pure water mainly illustrate differences arising from the composition of the binding materials. Thus the pure water results may be used to study the relative influence of cement composition on the degradation behaviour.
At present the most likely site for an intermediate level radwaste repository lies in a marl formation. Therefore, a standard marl groundwater has been defined for this study. The underlying analytical values have been measured at Oberbauenstock during a drilling campaign in 1987. The analysed water was contaminated by drilling fluid and attempts have been made to extrapolate the measured concentrations to zero contamination [19, Table 4].

Table 4: Chemical composition of raw materials used in this report. Values are given as % by weight of completely dry material.

Oxide	Cement HTS	Trass[1]	78.6 % HTS + 21.4 % trass[2]	Cement Sulfacem	
				selected[3] values	measured[4] range
CaO	68.1	5.4	54.7	62.0	62 - 63
SiO_2	24.1	57.3	31.2	20.5	20 - 21
Al_2O_3	2.6	20.1	6.3	4.0	2.8 - 4.2
Fe_2O_3	1.5	6.4	2.5	7.25	7.0 - 7.5
SO_3	2.1	0.2	1.7	2.75	2.5 - 3.0
K_2O	0.16	5.6	1.3	1.0	—
Na_2O	0.1	1.65	0.43	0.1	$\frac{1}{10}$ of K_2O[5]
MgO	0.7	1.32	0.83	1.2	—
$CaCO_3$	0.57	—	0.45	—	—
loss by ign.	—	2.3	0.5	—	—
Clinker composition:[6]					
C_3S	64.9			50.1[7]	45 - 50
C_2S	20.1			21.0[7]	20 - 22
C_3A	4.3			0[7]	0
C_4AF	4.5			19.1[7]	18 - 20
C_2F	—			—	0 - 2

[1]Values based on dry trass; $\sim$ 9 % of water not considered

[2]Mixture based on dry trass; corresponds to 100 parts of HTS and 30 parts of "wet" trass

[3]Values selected from measured range for use in the present study

[4]Range provided by manufacturer; actual values vary from batch to batch

[5]Assumption; value provided by manufacturer

[6]For nomenclature see Table 1

[7]calculated from selected values according to Bogue [5]

Table 5: Calculated composition of hydrated model components as taken from Table 4. Calculations are performed according to [2,3]. For the blended cement (HTS + trass), a comparison is made with the hydration model proposed by Glasser [4]. The calculations are based on a water to cement (+ trass) ratio of 0.43. Values are given as mmoles / kg of hydrated cement and as % by weight.

Model components	cement "HTS" + "wet" trass + water 100:30:52 (by weight)				Cement "Sulfacem"	
	present model		model of Glasser		present model	
	mmoles	% $^{w}/_{w}$	mmoles	% $^{w}/_{w}$	mmoles	% $^{w}/_{w}$
$C_3A_{0.725}F_{0.275}H_6$	401	15.8				
$C_3A_{0.17}F_{0.83}H_6$					384	16.3
$C_4A\bar{S}H_{12}$ (low-sulph.)	146	9.1			192	12.0
$C_4A_{0.786}F_{0.214}\bar{S}_{0.28}H_{12.72}$[1]			517	30.5		
$C_6A\bar{S}_3H_{32}$ (Ettringite)					16.1	2.0
$M_{5.3}AH_{(13.7)}$[2] (Hydrotalc.)			27.2	1.5		
$C_{1.39}SH_{1.39}$	3620	59.0				
$C_{1.31}SH_{(1.31)}$[2]			3627	57.0		
$C_{1.8}SH_{1.8}$					2386	46.2
CH (Portlandite)					1420	10.5
MH (Brucite)	144	0.8			208	1.2
KOH	196	1.1	(196)[2]	(1.1)	148	0.8
NaOH	97.2	0.4	(97.2)	(0.4)	22.4	0.1
$CaCO_3$	31.5	0.3	(31.5)	(0.3)	—	—
unused water	7211	13.0	(4844)	(8.7)	5560	10.0
maximum density	2030 kg/m^3		(2030 kg/m^3)		2090 kg/m^3	
minimum porosity	26 %		(~18 %)		21 %	

[1] Al_2O_3 replaced by $\sum Al_2O_3,Fe_2O_3$; H_2O replaced by $\sum H_2O,SO_3$

[2] not specified in Glasser's model; values assumed by analogy

The procedure for defining the standard marl groundwater composition is described elsewhere [43]. Here, only a short outline is given:

1. The values given in Table 6, column 1, define the basic water composition.
2. Temperature is assumed to be 25 °C, pCO_2 is assumed to be -2.0 [24]
3. Ca^{2+} and CO_3^{2-} are calculated from
   - saturation with calcite
   - $pCO_2 = -2.0$
   - charge balance
4. F^- is calculated from fluorite saturation
5. $H_2SiO_4^{2-}$ is calculated from quartz saturation

The standard marl groundwater composition given in Table 6, column 2, has been calculated according to this procedure, the values given in parentheses (column 3) indicate measured concentrations of a marl groundwater contaminated with drilling fluid.

Table 6: Standard marl groundwater used in the present study. The procedure for defining this standard groundwater is briefly outlined in the text. Total concentrations are given as mmoles/litre, the charge has to be balanced with the proton (H^+). The values given in parentheses indicate measured concentrations of a groundwater contaminated with drilling fluid.

Component	Measured total concentrations	Calculated concentrations (T = 25 °C)	Measured
Na^+	121.9		
K^+	0.47		
Ca^{2+}		5.58	(2.37)
Mg^{2+}	0.66		
Sr^{2+}	0.09		
Cl^-	76.16		
F^-		0.22	(0.6)
NO_3^-	1.61		
CO_3^{2-}		4.57	
SO_4^{2-}	26.4		
$H_2SiO_4^{2-}$		0.10	(0.1)
pH		7.27	
Alkalinity		4.22	
Ionic strength		0.15	
		Saturation indices	
		Calcite :	-0.02
		Quartz :	-0.02
		Fluorite :	-0.04
		Celestite :	-0.26
		Gypsum :	-0.52
		Dolomite :	-0.91

5 The mixing tank model

A condensed description of the mixing tank model and some preliminary results on the degradation of a standard Swedish Portland Cement have already been published elsewhere [20]. However, the mixing tank model used to describe the degradation of hydrated cement is outlined more detailed in the following section.
After a rapid initial period of hydration (typically several weeks) the hydration of portland cements continues slowly over a long time period (tens of years or even more), depending on the availability of hydration water, on the initial inventory, on the cement grain size etc. Phase transformations within the hydrated cement may continue over much longer time periods and as already mentioned, it is not clear whether a thermodynamically stable state will ever be reached. Within a repository, degradation of the cement will start soon after emplacement and resaturation and, therefore, degradation may start while hydration- and phase transformation processes still continue. A complete degradation model would therefore require the simultaneous description of hydration- , phase transformation- and dissolution-processes. The model should also be capable of considering different reactions going on simultaneously at different places within the cement structure. This would also require the consideration of transport processes. Such models are not in a practically usable state at present.
In order to give an estimate of how the total chemical inventory of a cement structure evolves with time in a given groundwater environment, a simple mixing tank model was developed. The model is based on the following simplifying assumptions:

1. The cement is fully hydrated and the phases present are considered to be in a state which can be modelled using the concepts of thermodynamic equilibrium.

2. In a first approach only a few phases are considered, namely : CSH–gel, $Mg(OH)_2$, KOH, NaOH and $Ca(OH)_2$ (cf. Table 5). For aluminate-, iron- and sulfate bearing phases (e.g. Ettringite), thermodynamic data are not yet available. These phases are not included in the present version of the model.

3. The time period to reach equilibrium between cement and leachant is short, compared to the time required to replace the leachant.

5.1 Calculation procedure for the mixing tank model

The calculation procedure for the mixing tank model is divided into several steps:

1. A normalised quantity (1 kg) of hydrated cement is equilibrated with a volume of the leaching solution. At the beginning of the procedure this volume is calculated from the minimal total porosity of the cement (cf. Table 5), which in fact is the difference between total water in the system and that used up by the hydration process.
   Example: The cement + trass mixture given in Table 5 has a density of 2030 kg/m^3 and a porosity of 26 %. Therefore, the volume of 1 kg of hydrated mixture is $0.493 \cdot 10^{-3}$ m^3.

Assuming a density of 1.0 for the unused hydration water, the volume of the leachant is $0.26 \cdot 0.493 \cdot 10^{-3}$ m^3/kg = $0.128 \cdot 10^{-3}$ m^3/kg.
The equilibrium calculations are performed with the geochemical speciation code MINEQL, assuming that the chemical inventory of the system is distributed homogeneously. Two kinds of solids have to be considered. Slightly soluble phases (CSH–gel, $Ca(OH)_2$, $Mg(OH)_2$ etc.) are treated in the usual way using the solubility product of the solid. The concept of solubility products is, however, not applicable to highly soluble phases like NaOH and KOH. A very high solution concentration and complete dissolution into the original pore solution would be the consequence, which, in fact is not observed ([3], page 30). For these phases it is assumed that a certain percentage of the inventory (availability parameter) dissolves in the pore solution. This assumption takes into account the fact that highly soluble alkali hydroxides may be incorporated into slightly soluble phases like $Ca(OH)_2$ or silicates, may be sorbed on the gel surfaces or may be just prevented from the contact with the solution.

2. From the equilibrium calculations (step 1) the quantities of dissolved solids are known. It is also checked whether new phases (e.g. $CaCO_3$, CaF_2, $CaSO_4$ etc.) become oversaturated and thus will precipitate. It is assumed that such precipitation is distributed homogeneously over the whole cement volume (in reality it is likely that "fronts" of precipitates will form). However, the new inventory of model solids is calculated based on the quantities of dissolved/precipitated solids. According to the dissolution model for CSH–gel, the thermodynamic properties of the remaining hydrated calcium silicates are recalculated. Using densities and quantities of dissolved/precipitated solid phases, the change of the total porosity is also calculated, but the quality or the availability of this porosity is not taken into account (e.g. changes in permeability or pore diameters).

3. The equilibrated solution is removed from the system and is replaced by a fresh volume of leaching solution.

This procedure (steps 1 to 3 are further designated as a water exchange cycle) is repeated until the whole inventory has completely leached out. As an example of how relevant parameters may change as a function of the cycle number, some of these parameters are given in Table 7, calculated after selected cycle numbers. The advantage of the proposed procedure is its simple application. Equilibrium codes are well established and are easy to handle. It is just a question of book-keeping and file organisation to run a speciation code thousands of times. In fact, not every single cycle is calculated. Hundreds of cycles may be jumped over by assuming "constant" chemical conditions, if the critical parameters (thermodynamic properties of CSH–gel, amount of phases still present, porosity) do not change very rapidly. The error introduced by this simplification is small compared to the uncertainty introduced by the thermodynamic approach and by the mixing tank approach.
Some disadvantages will limit the use of the mixing tank concept. Most restrictive is the fact that the temporal evolution must be expressed in terms of cycles rather than in terms of real time. Independent informations have to be known to relate cycle time with real time (e.g. the amount of groundwater intruding into the system per unit time). The mixing tank model describes the chemical evolution under constant, fixed boundary conditions which may be valid for a small "reference" volume. The kinetic, space and time dependent process of mass transport in the pore

solution and also large scale inhomogeneities (spatial and temporal distribution of processes) are not considered.

Table 7: Evolution of relevant parameters during the degradation of the cement + trass mixture (Table 5) in standard marl groundwater. The values are given after the calculation of the cycle indicated in the top row. CSH–gel is completely leached after 6650 cycles.

Parameter	Selected number of Cycles					
	1	100	523	1097	4413	6650
C/S - ratio	1.39	1.33	1.05	0.90	0.24	0
Porosity (%)	26.5	28.0	28.4	31.0	40.1	46.5
ml of leachant per kg of cement (porosity)	130	138	140	153	197	229
pH	12.9	12.4	12.0	11.2	10.3	7.4
$\log \hat{K}_{so}^{Ca(OH)_2}$	-5.57	-5.65	-6.65	—	—	—
$\log \hat{K}_{so}^{CaH_2SiO_4}$	-8.16	-8.16	-8.16	-7.95	-8.01	—
$\log \hat{K}_{so}^{SiO_2}$	—	—	—	-4.66	-2.87	-2.70

6 Results and discussions

6.1 Degradation of model cements

The degradation of the cement blend HTS + trass (100/30 $^{w}/_{w}$), further designated as "HTS" and of the sulfate resistant Sulfacem cement ("SUL") have been modelled in pure water ("WAT") and in standard marl groundwater ("MAR") (Table 6) using the mixing tank model described in section 5. The chemical evolution of the pore solution as a function of the number of water exchange cycles is shown in Figures 7 to 10. Edges and vertical parts of the curves within Figures 7 to 10 (and also in subsequent figures up to Figure 17) are induced by complete dissolution of existing and/or precipitation of new solids and are characteristic for the mixing tank model applied.

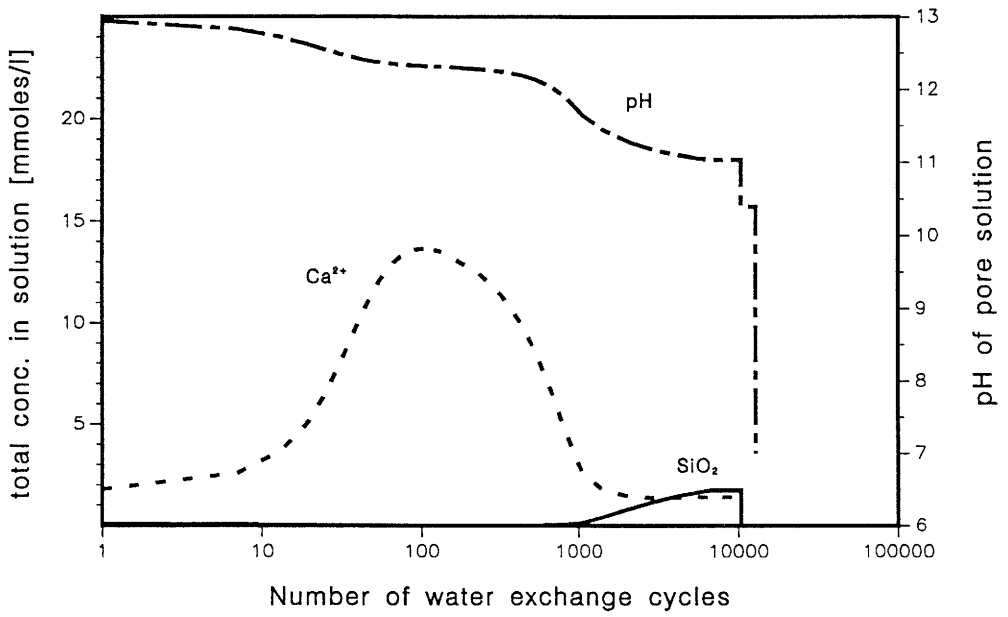

Figure 7: Degradation of cement blend "HTS" in pure water (T = 25 °C)

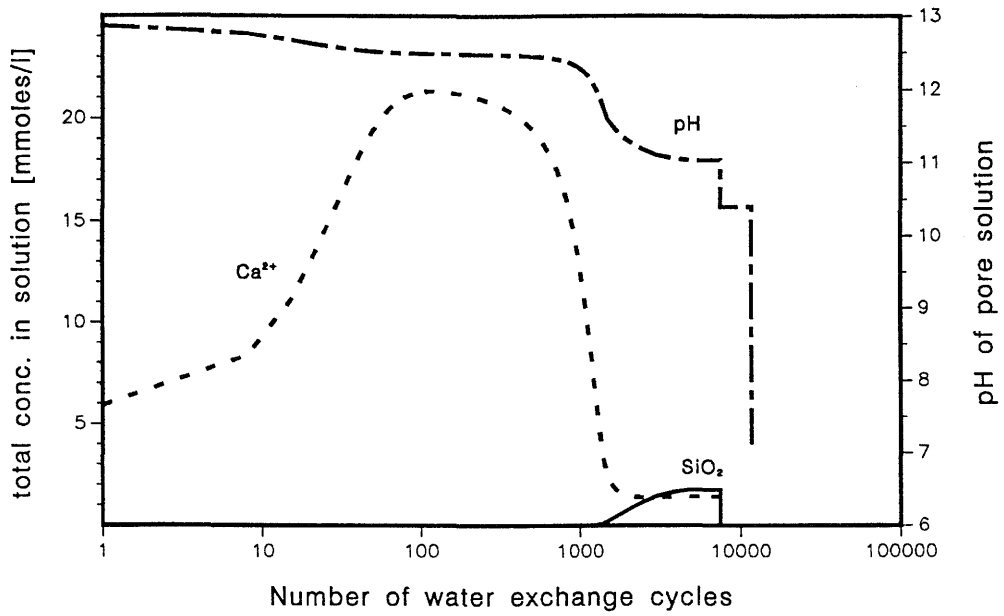

Figure 8: Degradation of sulfate resistant cement "SUL" in pure water (T = 25 °C).

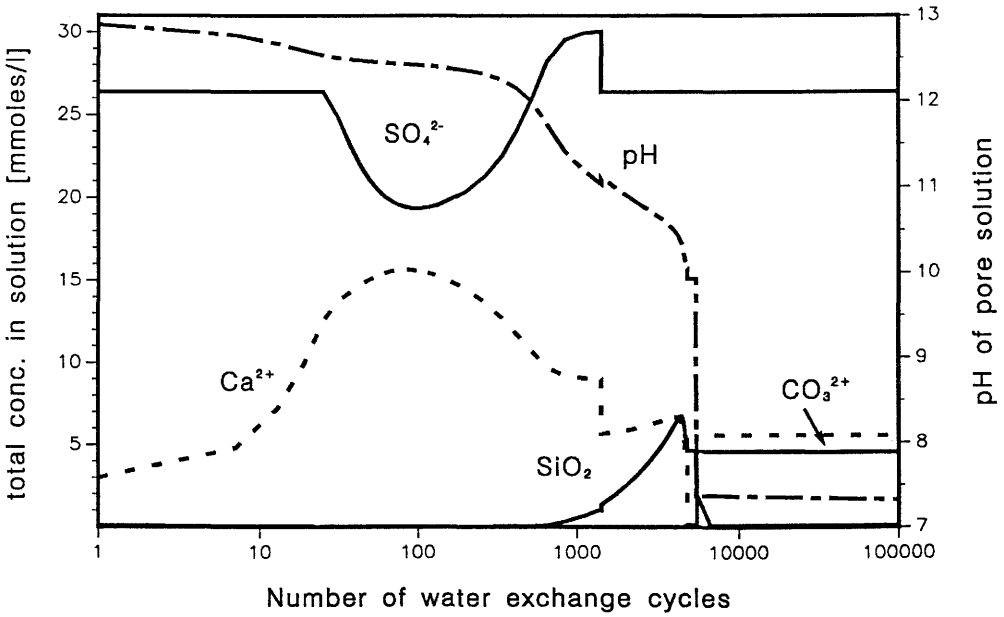

Figure 9: Degradation of "HTS" in standard marl groundwater "MAR". After 6650 cycles calcite is the only model solid present (T = 25 °C).

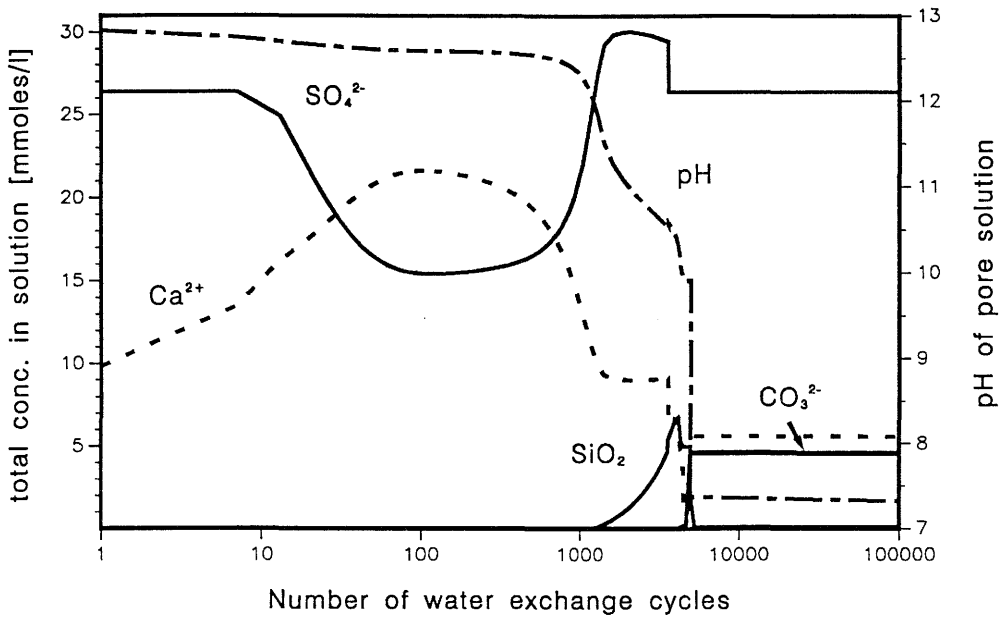

Figure 10: Degradation of "SUL" in standard marl groundwater "MAR". After 5310 cycles calcite is the only model solid present (T = 25 °C).

6.1.1 Degradation in pure water

The results are qualitatively similar to those recently published for the degradation of a standard Swedish portland cement in a carbonate–rich groundwater [15]. Several stages of degradation may be distinguished:

In a first stage of degradation the pore solution is dominated by the highly soluble alkali hydroxides NaOH and KOH (see also section 5.1). It is still an open question as to how much of the total alkali is dissolved in the initial pore water solution of the fresh cement and at what rate the remaining alkali dissolves during the subsequent degradation process. Experimental results of Glasser [6] and of Andersson [21] (compiled in [3]) indicate a retention ("sorption", "incorporation") of sodium and potassium by hydrated cement minerals. The nature of this retention is not well known at present. It seems that the portion of dissolved alkalis depends on the alkali content of the cement, on the W/C ratio and on the nature and portion of cement additives. In general the pore water solution is found to contain some 20 to 30 % [3] of the total alkali, the rest being retained by the solid phases. The portion of dissolved alkali may be as low as 2 % of the total in the case of K^+ in silica fume/cement blend. Generally, the retention in the solid matrix is more pronounced for sodium.
If cements are hydrated using W/C ratios above 2 by applying continuous mixing, all available alkali hydroxides are dissolved in the mother liquid after 6 month [22], indicating that alkali retention in cements is not a question of slightly soluble alkali bearing cement minerals.

However, for the present study it was assumed that 5 % of the remaining NaOH and KOH dissolve into the pore solution during each cycle. It is a consequence of this 5%–choice that up to around 80 cycles the pore solution chemistry is dominated by NaOH and KOH.

In a second stage (from $\sim$ 100 up to $\sim$ 1000 cycles) the pore solution is dominated by saturated "$Ca(OH)_2$". If the remaining CSH–gel exhibits a high C/S ratio (C/S $>\sim$1.8; cement "SUL") the solubility of this "$Ca(OH)_2$" is very similar to that of pure portlandite (cf. Figure 4 section 3), which means that the pH is $\sim$ 12.5 and $[Ca^{2+}]_{tot} \approx$ 22 mmoles/l. If the CSH–gel has a lower C/S ratio (C/S $<\sim$1.4; blend "HTS") the pH will be below 12.5 and $[Ca^{2+}]_{tot}$ will be below 20 mmoles/l, according to the dissolution model for CSH–gels. Silica concentrations are generally low ($[SiO_2]_{tot} < 0.03$ mmoles/l) within stage 1 and 2.

In a third stage (from $\sim$ 1000 up to a few thousands of cycles) the C/S ratio of the CSH–gel will drop below 1. The pH of the solution drops continuously down to pH $\approx$ 11, $[Ca^{2+}]_{tot}$ drops to a 1 to 5 mmoles/l level and $[SiO_2]_{tot}$ is increased to 2 to 6 mmoles/l. If pure water is used as the degrading solution the system reaches a point of congruent dissolution ($C/S_{solution}$ = C/S_{solid}) at

- C/S = 0.81,
- pH = 11.1,
- $[Ca^{2+}]_{tot}$ = 1.4 mmoles/l and
- $[SiO_2]_{tot}$ = 1.7 mmoles/l.

A congruent dissolution behaviour is not found if "MAR" is used as degrading solution. If CSH–gel has dissolved completely, the remaining $Mg(OH)_2$ dissolves at a pH of 10.4, after which the pH rapidly drops to 7.

6.1.2 Degradation in standard marl groundwater

Qualitatively, the three stages of degradation are also observed if the degradation is modelled in "MAR" solution, but some additional processes have to be considered. The standard marl groundwater contains anions (SO_4^{2-}, CO_3^{2-}, F^-) which may react with the calcium released from CSH–gel to form new solids e.g. calcite, gypsum, fluorite. The speciation calculations show that brucite ($Mg(OH)_2$), calcite ($CaCO_3$), gypsum ($CaSO_4$) and fluorite (CaF_2) are oversaturated and thus will precipitate (presuming that supersaturated states do not occur) if "MAR" solution is in equilibrium with the cement minerals.
The amounts of the model solids as a function of cycles are shown in the Figures 11 and 12 for the degradation of "HTS" in "WAT" and "MAR". The figures show the percentage (on a molar base) of the original inventory of the cement ("$Ca(OH)_2$", $CaCO_3$, $CaSO_4$ and CaF_2 are based on "$Ca(OH)_2$" = 100 %).

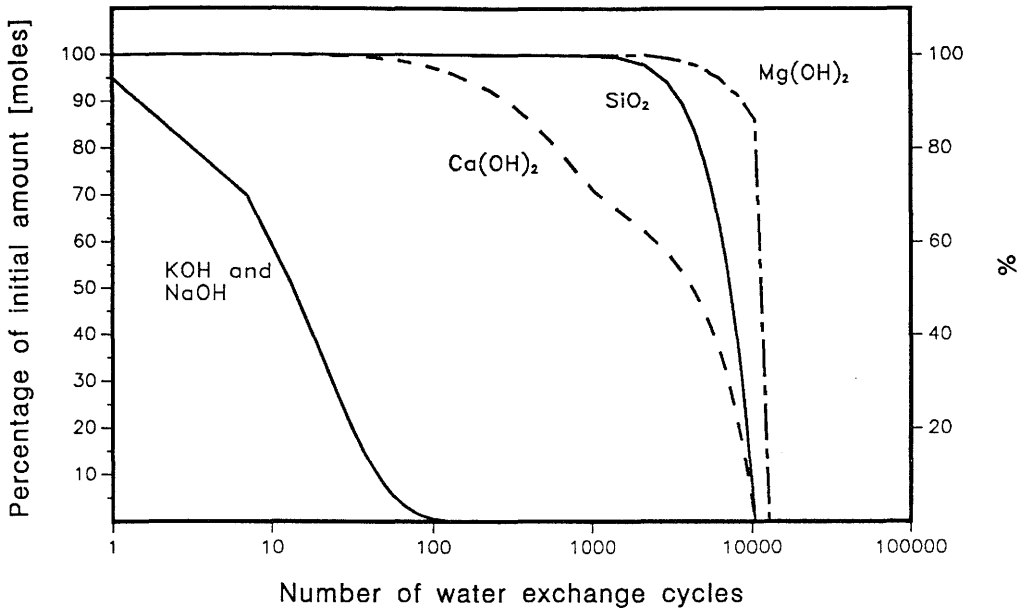

Figure 11: Degradation of "HTS" in pure water. The amounts of model solids per unit mass are given as a function of cycles. The percentage scale is based on the initial molar amounts present in the cement (T = 25 °C).

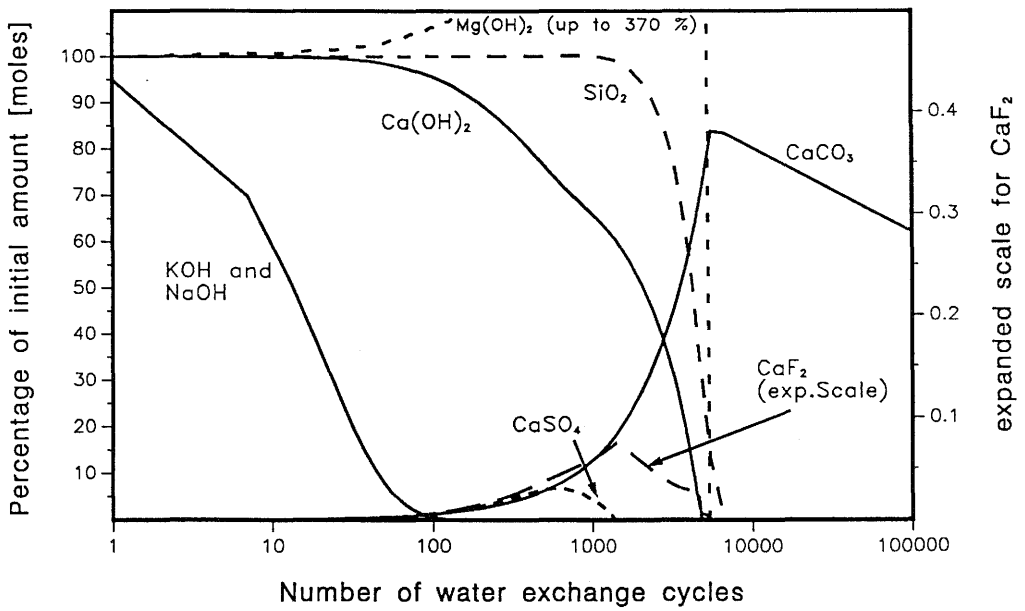

Figure 12: Degradation of "HTS" in standard marl groundwater "MAR" (T = 25 °C). The amounts of model solids per unit mass are given as a function of cycles. The percentage scale is based on the initial molar amounts present in the cement. Ca bearing phases are based on "$Ca(OH)_2$"$_{total}$ = 100 %. Due to the low values CaF_2 is associated with the expanded right axis.

Brucite:

$Mg(OH)_2$ is precipitated as long as the pH stays above pH $\simeq$ 10.4. Therefore the amount of solid $Mg(OH)_2$ is increased to about 370 % of its original value. The maximum value is reached at $\sim$ 4400 cycles (combination "HTS"/"MAR").

Calcite:

"MAR" was defined assuming calcite saturation (cf. Table 6) and therefore $CaCO_3$ will precipitate as long as the pH is above $\sim$ 7.3 or as long as $[Ca^{2+}]_{tot}$ is above $\sim$ 5.6 mmoles/l. Nearly 83 % of the original "$Ca(OH)_2$" is transformed to calcite at $\sim$ 6650 cycles. This transformation approximately halves the "lifetime" of the CSH–gel (compared to the dissolution in "Wat") and therefore CO_3^{2-}– concentration in the groundwater is avery important parameter.

Gypsum:

SO_4^{2-} shows an interesting behaviour as can be seen from Figures 9 and 10. Above a $[Ca^{2+}]_{tot}$ level of $\sim$ 13.8 mmoles/l gypsum begins to precipitate and $[SO_4^{2-}]$ is decreased, depending on the actual release of Ca^{2+} into the pore solution. About 7 % of the original "$Ca(OH)_2$" is transformed into $CaSO_4$ at $\sim$ 650 cycles ("HTS" / "MAR"). Due to a changing C/S ratio of the CSH–gel the $[Ca^{2+}]$ level drops below $\sim$ 10 mmoles/l and gypsum starts dissolving. For a period of $\sim$ 900 cycles $[SO_4^{2-}]$ is higher than in the original marl groundwater and $[Ca^{2+}]$ remains nearly constant at $\sim$ 9 mmoles/l. Gypsum dissolves completely after $\sim$ 1400 cycles, accompanied by a sharp drop in $[Ca^{2+}]$ and $[SO_4^{2-}]$ ("HTS"/"MAR"; Figure 9).

Fluorite:

The behaviour of fluorite is similar to that of gypsum but on a 100 fold lower level. about 0.1 % of the original "$Ca(OH)_2$" is transformed into CaF_2 at $\sim$ 1400 cycles ($\sim$ 3.8 mmoles/kg of hydr. cement are precipitated) and during the subsequent dissolution of CaF_2 the F^- concentration is increased above the level of the original "MAR"–solution. Fluorite dissolves completely after some 4780 cycles.

6.1.3 Comparison of "lifetimes"

To some extent the pH of the pore solution may serve as an indicator for the "lifetime" (given in cycles) and of the evolution of the solid phases of the cement. Figure 13 shows the pH of the pore solution modelled for any combination of cement and degrading solution. In the present study the "lifetime" of a cement is defined as the cycle number at which CSH–gel has dissolved completely. The so defined "lifetimes" are compiled in Table 8. In pure water the cycle number at which CSH–gel has dissolved completely strongly depends on the amount of silica present in the cement. The amount of total "$Ca(OH)_2$" (the C/S ratio) determines the pH–level of the pore water at a given cycle. The "SUL" cement, which starts degrading at a high C/S ratio (2.4), produces a higher pore solution pH than the "HTS" cement (C/S = 1.39) up to $\sim$ 2000 cycles

(cf. Figure 13). The absolute "lifetime" of, and also the difference in "lifetimes" between the two cements decreases if the degradation is modelled in "MAR" solution, but the difference in the pH levels is still present. From the reduction factors F_R in Table 8 it can be seen that the influence of the degrading solution properties is more pronounced than the influence of the cement composition.

The main parameter which determines the "lifetime" in "MAR" solution is the $[CO_3^{2-}]_{tot}$ level of "MAR". As pointed out before, $Ca(OH)_2$ from CSH–gel is transformed into $CaCO_3$ and, therefore, high CO_3^{2-} concentrations cause increased transformation of CSH–gel into $CaCO_3$ and CSH–gel with decreased C/S ratio. For CSH–gels with C/S $>$ 1 it is calculated that $[CO_3^{2-}]_{tot}$ of the leachant must be below $1.1 \cdot 10^{-5}$ M in order to prevent precipitation of calcite.
Its not clear at present, whether and to which extent the "lifetime" is influenced by SO_4^{2-}. This study does not take into account sulfate bearing phases like ettringite or low-sulfate (AFt–, AFm phases) and redox equilibria with S^{2-} and therefore the surprising behaviour of SO_4^{2-} and gypsum may be unique for the assumptions made for this study.

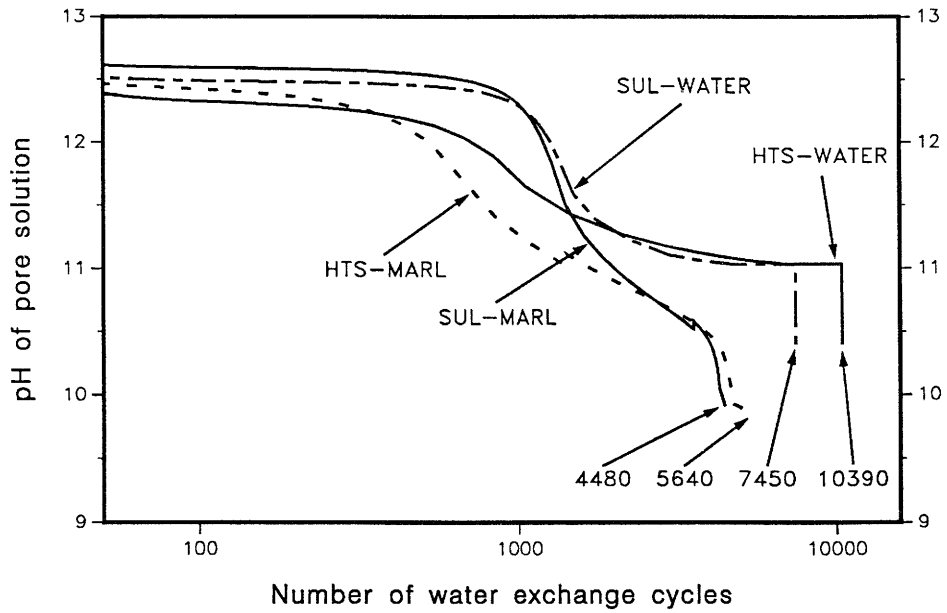

Figure 13: "Lifetime" of "HTS" and "SUL" degraded in pure water ("WAT") and in marl groundwater ("MAR"). The pH of the pore solution serves as an indicator for the evolution of the model solids. The numbers indicate the cycle at which CSH–gel has dissolved completely (T = 25 °C).

Table 8: "Lifetime" of "HTS" and "SUL" degraded in "WAT" and in "MAR".

The cycle number at which CSH–gel has dissolved completely is given. The reduction factors F_R specify the reduction in "lifetime" by changing the solution from "WAT" to "MAR" and by changing the cement from "HTS" to "SUL".

	"WAT"	"MAR"	Reduction factor F_R "WAT" $\longrightarrow$ "MAR"
"HTS"	10390	5460	1.9
"SUL"	7450	4480	1.7
Reduction factor F_R "HTS" $\longrightarrow$ "SUL"	1.4	1.2	

6.2 Conclusions: Cement degradation

The following conclusion are drawn from the results presented in the previous subsection:

1. The "lifetime" (as defined on page 26) of a cement strongly depends on the chemical composition of the degrading groundwater. Carbonate is likely to be the most important parameter due to the transformation of CSH–gel into calcite.

2. Concerning the "lifetime", the composition of the cement is less important than the composition of the degrading solution. For a given degrading solution a high silica portion increases the "lifetime" but decreases the pH level of the pore solution.

3. The pH, one of the most important parameters of the pore solution, is determined by the C/S ratio of the cement. Cements with high initial C/S ratios (C/S $>$ 1.8; unblended cements, e.g. "SUL") produce pore solutions with higher pH levels over long time periods than low C/S ratio cements (cements containing additives, e.g. "HTS").

4. Criteria for selecting specific cements should not be based on expected "lifetime", but on the consequences of the predicted pH – regime on radionuclide release.

6.3 Uranium solubility in the pore water of degrading cement

For the present study uranium was selected as a representative for actinides exhibiting a complex speciation behaviour. Nuclides different from U, such as Cl, I, Sn, Se, Pd, Ni, Tc and the Np – chain will probably contribute much more to the final dose to man if the whole model chain from the repository to men is considered. These nuclides may be more relevant and should therefore have a higher priority than uranium. However, it was not the main aim of this exercise to provide definitive solubilities of specific radionuclides nor to perform site specific modelling, but rather to show that such modelling is feasible and to address the problems encountered during the modelling work.

Uranium is qualified for serving as a "pilot"-nuclide for several reasons. Many soluble complexes and their formation constants are known for U. A lot of slightly soluble uranium bearing solids are known which may produce U solubilities differing by many orders of magnitude (depending on the leachant). In addition, dissolved (and also solid) U is present in four oxidation states (U(III) to U(VI)) which would enable to study the influence of varying electrochemical potentials. In order to model solubility, a solid has to be defined stoichiometrically and its thermodynamic properties have to be known. It is not clear, into which solid phase uranium enters if radioactive waste (for example ion exchange resins) is solidified with cement. Therefore model calculations have been performed using several solid uranium phases, in particular

- UO_2, U_4O_9, U_3O_8 as oxidic phases with "averaged" oxidation states of 4, 4.5 and 5.33 respectively.
- $USiO_4$ as a silica bearing solid and
- $CaUO_4$ as a Ca bearing solid

A compilation of the thermodynamic database used for this study (MINEQL/PSI) is given in [23]. Some 15 to 20 solid uranium phases also included in this database, have not been considered (e.g. solids producing unrealistic high concentrations for the given leachant or different modifications of the same solid).
A fixed redox potential of ~ -300 mV (pE = - 5) has been chosen for all calculations presented in this section. This choice is based on the definition of pE in sediment groundwaters (for more detailed information see [24, page 271]). The influence of *varying* the redox potential is not investigated, this may be a topic for a subsequent, more detailed report on radionuclide speciation.
The modelling procedure was equivalent to the procedure applied for the degradation of non-contaminated cements (cf. section 6.1). An amount of the corresponding uranium phase was "added" to the hydrated cement and the solubility was then modelled by assuming thermodynamic equilibrium with cement and leachant.
Figure 14 shows the evolution of the total uranium concentration for different U–solids during the degradation of "HTS" in standard marl groundwater. In the high pH environment (for pore solution compositions see Figure 9) the calculated aqueous speciation of U is very simple, $U(OH)_5^-$ being the dominant aqueous complex in all systems considered. The total uranium concentration varies over more than 10 orders of magnitude from $\sim 10^{-4}$ M ($USiO_4$) to $7.4 \cdot 10^{-15}$ M

($CaUO_4$). Within stage 1 and stage 2 of cement degradation (see section 6.1) the uranium levels produced by the particular solids remain nearly constant, at higher degradation stages the trend is towards higher concentrations for U_3O_8 and $CaUO_4$ and towards lower concentrations for UO_2, U_4O_9 and $USiO_4$. If the degradation enters stage 3 the situation becomes very complex. Due to decreasing pH and $[Ca^{2+}]_{tot}$ the solubility of $CaUO_4$ is increased from 10^{-14} M up to molar levels. Due to the increased silica concentration within stage 3 the solubility of $USiO_4$ decreases from $\sim 10^{-4}$ M to $\sim 10^{-9}$ M. The solubility curves for UO_2 and U_4O_9 correspond to the pH curve (above $\sim$ 500 cycles the U_4O_9 - curve decreases less than the UO_2 - curve), whereas the curve for U_3O_8 increases with decreasing pH. The solubility behaviour of the latter three solids is not only a function of pH but also of the redox potential. A redox potential different from $\sim$ - 300 mV could lead to different shapes and levels of the solubility curves.
Figure 14 clearly indicates that several uranium bearing solids may serve as the thermodynamic stable phase during the degradation of the cement.
Lets assume that the phase $CaUO_4$ does not exist (the existence of this phase has to be investigated carefully) and that a thermodynamic equilibrium is established between the most stable uranium bearing phase, the cement minerals and the leachant. In this case UO_2 or U_4O_9 would be the most stable solid phases in the system up to $\sim$ 500 cycles (the curves for UO_2 and U_4O_9 are essentially coincident). From 500 up to 900 cycles UO_2 or $USiO_4$ would be stable, above $\sim$ 900 cycles $USiO_4$ would definitely be the most stable phase. If $CaUO_4$ exists, it determines the solubility of U up to $\sim$ 2900 cycles. At this point the curve intersects with the $USiO_4$–curve and above $\sim$ 2900 cycles $USiO_4$ becomes the stable phase.
The cumulative uranium leaching from the cement is obtained from the concentration of U, multiplied by the pore volume and the number of cycles. These results are compiled in Figures 15 to 17. Figure 15 gives an overview and covers a range from zero to 20 mmoles U/kg of hydrated cement (corresponding to $\sim$ 5000 ppm U in the cement). A more realistic range is shown in Figures 16 and 17, exhibiting the influence of leachant and cement composition on the cumulative leaching for different solids (a realistic U–inventory in the repository is indicated by the horizontal line). If U_3O_8 is used as the solubility limiting phase the total U–inventory will be leached out after a few cycles. If UO_2 or U_4O_9 (these two solid phases show nearly equivalent behaviour at the Eh conditions considered) are used as the solubility limiting phase it takes some hundred cycles to leach all U. If $CaUO_4$ is the stable phase very little U is leached during the first $\sim$ 500 cycles, afterwards all U escapes within a few cycles. A comparison of the curves shows nearly no influence of the cement composition (Figure 17) and only negligible influence of the leachant composition (Figure 16). However, it has to be noted that this independency on cement and on leachant composition is valid for U and likely for actinides exhibiting a similar chemical behaviour (e.g. Pu). For other radionuclides the cement composition may have a strong influence on the cumulative leaching, especially if the total solubility of the radionuclide in question is determined by sorption on cement rather than by slightly soluble solids (e.g. for I and Cl). Anions dissolved in the leachant (e.g. F^-, SO_4^{2-}) may form complexes or slightly soluble solids with some radionuclides and therefore increase or decrease their concentration, and subsequent, the cumulative leaching.

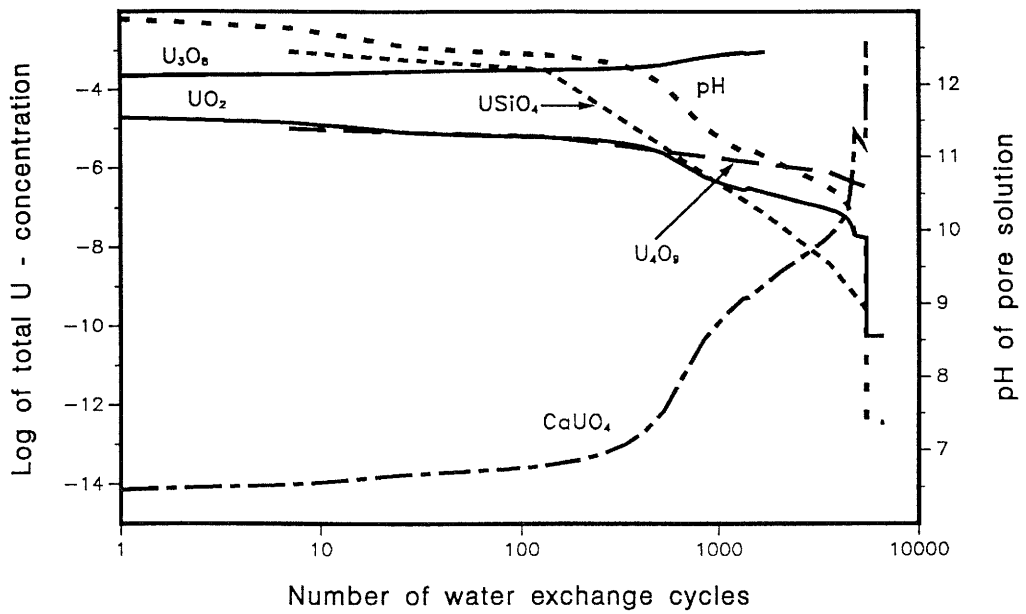

Figure 14: Total concentration of uranium in the pore water of "HTS" degrading in "MAR" solution calculated for several uranium bearing solids. For each solid a separate calculation is performed, assuming that there is no interference with other phases (T = 25 °C).

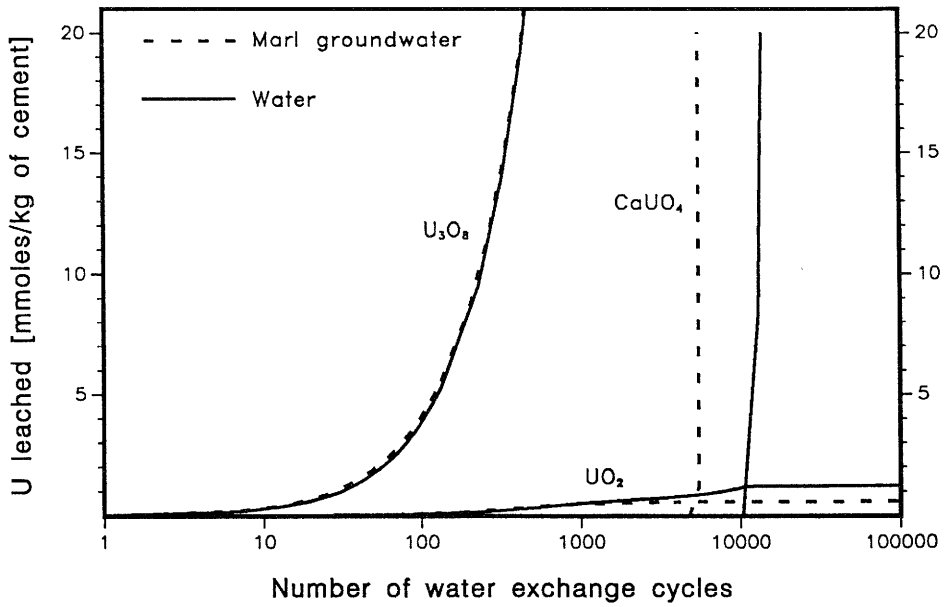

Figure 15: Cumulative leaching of uranium from cement "HTS" degrading in "MAR" and in "WAT" as a function of the number of cycles. The three sets of curves are calculated assuming the indicated solid being the only possible solubility limiting solid (T = 25 °C).

Solid line : degradation in pure water
Dashed line: degradation in standard marl groundwater

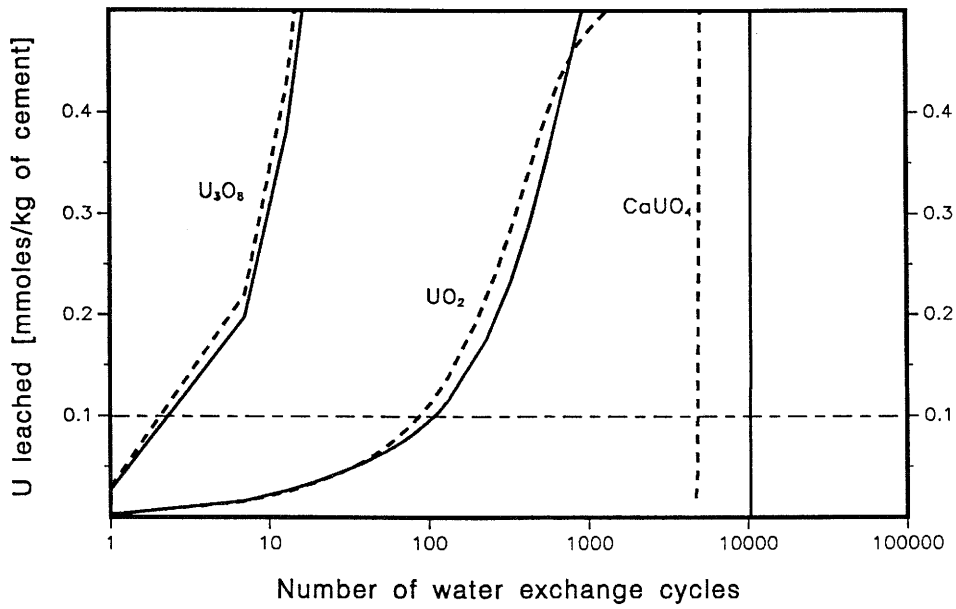

Figure 16: Cumulative leaching of uranium from cement "HTS" degrading in "MAR" and in "WAT" as a function of the number of cycles. The three sets of curves are calculated assuming the indicated solid being the only possible solubility limiting phase. The horizontal line indicates a realistic U – inventory of a cement based repository (T = 25 °C).

The figure is an expanded part of Figure 15.
Solid line : degradation in pure water
Dashed line: degradation in standard marl groundwater

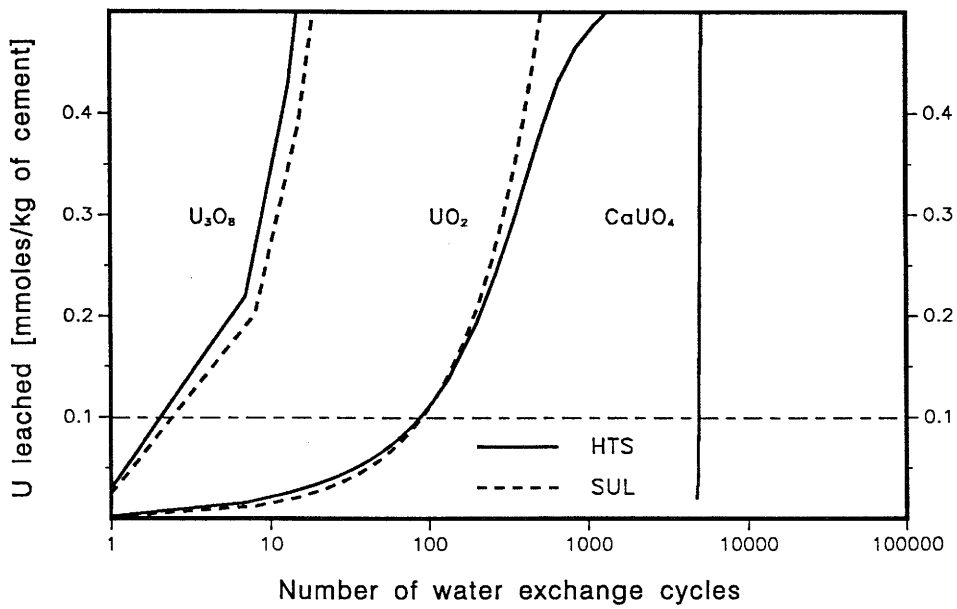

Figure 17: Cumulative leaching of uranium from cement "HTS" and from cement "SUL" degrading in standard marl groundwater "MAR" as a function of the number of cycles. The three sets of curves are calculated assuming the indicated solid being the only possible solubility limiting phase. The horizontal line indicates a realistic U – inventory of a cement based repository (T = 25 °C).

Solid line : degradation of cement "HTS"
Dashed line: degradation of cement "SUL"

6.4 Conclusions: Uranium leaching

The solubility of uranium in the pore solution of degrading cement may vary by several orders of magnitude (cf. Figure 14), depending on the properties of the solubility limiting phase. The cement—leachant systems considered in the present study produce U–solubilities of $\sim 10^{-14}$ M for $CaUO_4$ and solubilities around 10^{-4} M ($\pm$ 1 order of magnitude) for UO_2, U_4O_9, U_3O_8 and $USiO_4$. If solids like $CaUO_4$, which have very low solubilities, are formed during the hydration of cement, they could reduce the release of U from the repository for long periods of time. Investigations of Glasser [25] and Macphee [26] show, that recently discovered uranium bearing solid phases in the systems $CaO–UO_3–H_2O$ and $(UO_3,CaO)–SiO_2–H_2O$ may have very low solubilities. It is therefore of most importance to

- investigate the solid phases formed in the system uranium–cement and to
- determine their thermodynamic properties

Uranium solids formed during the hydration of cement may be subject of phase transformations and the question towards the kinetics and towards the final state of such transformations must be raised.
Uranium may be present in low concentrations compared to the solid phases comprising the hydrated cement. Concentration levels of 0.1 mmoles of U/kg of hydrated cement (average over whole repository) have been calculated from a possible repository inventory given in [27]. Those 0.1 mmoles/kg have to be compared with more than 3000 mmoles/kg of CSH–gel. If CSH–gel serves as a host for uranium, its solubility behaviour may rather be determined by the dissolution of CSH–gel than by the thermodynamics of a "pure" uranium solid. It has to be checked, whether the thermodynamic approach applied in the present study is valid or not. In the latter case different solubility models (for example a solid solution model) have to be developed.
The aqueous speciation of uranium was mentioned very briefly (section 6.3; page 29) due to its simplicity within the systems considered. In contradiction to the present results which are based on the MINEQL/PSI database, Bruno [28] recently found that $U(OH)_5^-$ is not a dominant species in a high pH–regime, even at reducing redox conditions. Bruno explains his solubility data by using the dissolved species $U(OH)_3^+$ and $U(OH)_4^0$. The application of Bruno's data would not strongly affect the cumulative leaching predicted by the present model. However, these data would certainly influence the uranium speciation and, therefore, the effects of sorption of U on cement (and on the host rock). Uranium species escaping from the repository will sorb on the surrounding host rock materials and the intensity of this sorption strongly depends on the speciation (especially on the charge of the species). It is therefore a prerequisite for further modelling of uranium speciation, to update the thermodynamic database and to check the quality of data relevant to the systems considered.

7 Conclusions and recommendations

7.1 General

The results show, that the presented model chain is capable of predicting the chemical evolution of a repository, even if a lot of assumptions and simplifications may limit its application to more general aspects. The influence of a variety of parameters (e.g. cement composition, groundwater speciation, redox conditions, thermodynamic properties of solid phases etc.) can be studied and the most relevant parameters determining the behaviour of a given system can be identified for further investigations. The use of the model also enables the modeller to define much more precisely the main aim of accompanying experimental programs and literature studies. The present model is a rough approach towards a complete understanding of the very complex cement system and essential parts of the model chain should be improved and refined in order to produce more dependable results. However, we felt that at first the different model parts had to be developed up to the minimal state required to calculate the whole model chain. Not till then it can be decided, whether its worthwhile to improve particular model parts or not.
The following subsections summarize the conclusions drawn from the different model parts and give some recommendations for further model development and accompanying experimental and/or literature work.

7.2 Hydration model

The solid phases comprising hydrated cements are well established and different hydration models assume similar classes of model solids (cf. Table 1, page 3). Variations of model solids within particular classes (Table 5, page 15) are not of most importance concerning the aim of the study and, therefore, have not a first priority. The present model assumes a solid solution of C_3AH_6—C_3FH_6 for iron and aluminium bearing phases and AFm/AFt—phases as sink for SO_4^{2-}. These assumptions have to be revised and refined. All magnesium is located in brucite ($Mg(OH)_2$); Mg–aluminates and Mg–silicates are not considered. This has to be checked also. It is recommended to replace the present hydration model by the more detailed model developed by Glasser et al. [4].
The final composition of blended cements is calculated based on the total inventory and on the "rules" applied for unblended cements, but the *real* final composition of hydrated blended cements has never been observed up today. It is not clear at present, whether the very long term hydration products of blending materials should be investigated or not. However, concerning the "present state of the art" of near field modelling such investigations would be a fine tuning procedure and therefore have a low priority.

7.3 Solubility model

The solubility data on CSH–gels found in the literature are represented in a satisfactory manner and the results are in good agreement with model results from Atkinson [29,30] and Glasser [4].

An advantage of the present model is its formalism in terms of "apparent solubility constants", which enables the direct implementation into common geochemical speciation codes. The solubility model concentrates on CSH–gels as the dominant phase, other important phases such as Al, Fe, Mg or SO_4^{2-} bearing phases are not considered within the present version. It is obvious that a comprehensive solubility model for hydrated cement must include these phases, otherwise the behaviour of important species like SO_4^{2-} cannot be understood (cf. Figures 9 and 10 and also page 27). It is foreseen to include these phases in a further development of the solubility model with first priority.
Attempts to experimentally test or to "validate" a solubility model for CSH–phases have been performed by Atkinson [30]. He simulated different leaching states by performing the measurements at different leachant/cement ratios and found reasonable good agreement between model predictions and experiments.
We believe that the solubility properties of CSH–gels are understood to an extent which enables the modelling of the general dissolution behaviour of the gels. It is therefore recommended to concentrate further theoretical and experimental work on specific topics (e.g. behaviour of alkali hydroxides, sulphur chemistry, redox properties etc.) and on (site) specific cements. This type of information is required for fine tuning of the models if real and site specific cement systems have to be modelled.
Experimental work has to be set up very carefully in order to get unequivocal answers. A main problem arises with the time available for an experiment in combination with the thermodynamic approach (assuming a stable state at infinite time) made within the models. A recently started experimental program [31] therefore concentrates on investigations of artificially "aged" (in the sense of "leached for a long period of time") HTS cement. Solubility–, sorption–, diffusion– and hydraulic properties are investigated.

7.4 Degradation of cement systems

The "lifetime" of hydrated cements is firstly determined by the composition of the leachant and only secondly by the composition of the cement itself. Concerning the leachant, the concentrations of anions (e.g. CO_3^{2-}, SO_4^{2-}, F^-) forming slightly soluble solids with the cations of the cement (Ca^{2+}, Mg^{2+}) are of most importance. These anions may transform the hydrated cement minerals into less soluble phases, exhibiting properties (for example sorption or retention of radionuclides) different from the cement minerals. For a given leachant, the "lifetime" of a cement is mainly determined by its silica content and the relative time period of high pH conditions (pH $\geq$ 12) is determined by the C/S ratio of the CSH–gel.

The present simple mixing tank model accounts for changes in the total porosity of the cement due to dissolution and/or precipitation of solids. It does, however, not account for the important changes in physical properties like diffusion parameters or permeability. In reality a repository will be leached by diffusive and/or advective transport of solutes and fronts with high gradients of physical and chemical properties may form during leaching. Fronts of precipitated solids may decrease porosity and permeability and may thus slow down the leaching of the remaining parts of the repository. This means that certain parts of a repository may be leached to a large extent, while other parts are still in a unleached state. It is not clear, which parts of the total porosity

are available to which processes and how the "available" porosity evolves with time (problem of varying pore size distribution). The description of the evolution of the pore size distribution requires a lot of material specific information such as W/C ratio, hardening conditions, stress history, shrinkage/swelling properties, drying/resaturation cycles etc., and it seems very difficult to work out all the relevant processes needed for a comprehensive model description. Therefore, we think that problems concerning the evolution of pore size distribution and related physical properties should rather be tackled experimentally than by theoretical models. A first experimental attempt is made in the experimental program mentioned above [31].
The concept of cycles, as proposed in the mixing tank model, cannot give answers in terms of *real* time except if the water infiltration into the system is very slow and completely dominated by the surrounding rock formation. However, spatial and temporal distribution of degrading processes will be the normal case and results concerning the *real time* evolution can only be obtained by coupling the chemical degradation models with transport models. Very first and simple coupled model calculations indicate, that the present state of available coupled codes would require too much of computer time to solve a problem of reasonable size [32,20]. Yeh and Tripathi [33] investigated and compared several coupled codes and concluded, that iterative coupled transport/speciation codes are best suited to solve realistic problems. At present it seems that coupled codes are the best way to proceed in the development of comprehensive cement degradation models. We agree with the conclusions of Yeh and Tripathi [33] and we recommend to focus further model development on the simplification of coupled transport/speciation codes of the *CHEQMATE*–type [34].

7.5 Radionuclide speciation

Important parameters determining the solubility behaviour of radionuclides in degrading cement have been identified by modelling the solubility of uranium as a complex example. Basically, the conclusions drawn from the behaviour of uranium are applicable to other radionuclides which are more relevant to radioactive waste disposal. Specific conclusions concerning particular nuclides may be worked out by using the present model.

The results clearly indicate that the chemical and thermodynamic properties of the uranium bearing phases are of key importance. In particular the solubility limiting phases and their thermodynamic properties have to be identified properly. This may require a lot of additional experimental and/or literature work. Two basically different cases can be distinguished:
In the favourable case the solubility limiting solid is a well-defined single phase. Its thermodynamic properties may be determined by experiment or estimated by chemical analogy.
In the unfavorable case no well-defined and no unequivocal phases are formed during the hydration of cement. This case is more plausible if the small amounts of radionuclides present are compared with the large amount of phases comprising the matrix. It is likely that one can start from the principle that uranium is finely distributed over a variety of matrix phases (CSH–gel, portlandite, aluminates etc.) as a solid solution. Then the well-defined thermodynamic approach becomes questionable, since the solubility of U will be determined by the degradation of the solid "solvent" rather than by independent equilibria of pure uranium bearing solids. If necessary, a modified solubility model based on solid solution theory has to be developed in order to

model the release of uranium. However, the basic questions must be answered by experiments. For this reason the investigations on uranium bearing solids mentioned above [25,26] have to be followed very carefully.
Certain conditions (low amounts of radionuclides, high sorption capacity) may cause that sorption on hydrated cement minerals becomes a dominant effect and thus will determine the release of radionuclides. Appropriate (sorption-) models should be developed and the required basic data should be gathered.

The speciation of dissolved uranium complexes at the extreme pH conditions in cement pore solution has not been investigated much in the past, but it is almost certain that hydroxide complexes will dominate the speciation. However, the discrepancy between the present results (all dissolved U is located in $U(OH)_5^-$) and the recent findings of Bruno [28] ($U(OH)_3^+$ and $U(OH)_4^0$ are the dominant aqueous species) indicate, that basic questions concerning the U–speciation in a high pH–regime are still open.
Occasionally it is stated that the high pH–regime in cements decreases the solubility of "radionuclides" and therefore high pH cements (unblended cements) are best suited for matrix and construction materials. This may be true for selected nuclides (e.g. Th) but the solubility tables from Pourbaix [35] and Baes & Mesmer [36] indicate that these statements must not be generalised. It depends on the hydroxide complexation of the particular radionuclide, whether a very high pH is favourable or not and the best conditions have to be optimised for each given system separately.
Summarised, it is recommended to revise and to further evaluate the thermodynamic databases with first priority. These databases are the heart of any modelling work involving quantitative chemical properties and should therefore be in a best possible condition.

A possible influence of minor components (inorganic, organic) dissolved in the leachant or in the cement pore solution on the solubility/speciation of radionuclides is not discussed within the present study. It is not expected that traces of inorganic components will affect radionuclide speciation. An exception could be traces of redox components (e.g. the sulphur system in slag cements) which could oxidize or reduce redox sensitives radionuclides (due to local inhomogeneities in the bulk Eh condition or due to kinetics). Additionally the rôle of organic complexants is still an open question. Organic ligands may be formed during degradation of organic matter included in the waste (e.g. ion exchange resins), but it is not known which degradation products actually will form. A recent published literature review [37] shows, that the complexing ability of organic ligands may dominate the aqueous speciation of radionuclides, especially at very low concentration levels of the nuclide in question. Therefore a possible strong influence of organic ligands has to be checked before the models and databases concerning the "inorganic" speciation are developed further.

Acknowledgements

I would like to thank Prof. F.P.Glasser, Prof. R.Grauer, Dr. J.Hadermann, Dr. P.Zuidema and Dr. I.G.McKinley for their critical review of this report. I specially wish to thank Dr. J.Hadermann for a lot of productive and critical discussions during the development of the various model parts. Partial financial support by NAGRA is gratefully acknowledged. The final layout of this manuscript performed by R.Bercher is also gratefully acknowledged.

References

[1] **Project Gewähr 1985**
Nuclear Waste Management in Switzerland:
Feasibility Studies and Safety Analyses
Nagra (National Cooperative for the Storage of Radioactive Waste)
Project Report NGB 85-09 (Baden, Switzerland, 1985)

[2] **Berner U. R.**
Modelling porewater chemistry in hydrated cement
Mat. Res. Soc. Symp. Proc. Vol. 84 (1987) p. 319

[3] **Berner U. R.**
Radionuclide speciation in the porewater of hydrated cement.
I. The hydration model
EIR Internal Report, TM-45-86-28 (Würenlingen, 1986)

[4] **Glasser F. P. , Macphee D. , Lachowski E. E.**
Modelling approach to the prediction of equilibrium phase distribution in slag-cement blends and their solubility properties
Mat. Res. Soc. Symp. Proc. Vol. 112 (1988) p. 3

[5] **Bogue H. R.**
Calculation of the compounds in Portland Cement
Ind. Engng. Chem. Analytical Edition 1 (4) (1929) p. 192

[6] **Glasser F. P. , Angus M. J. , McCulloch C. E. , MacPhee D. , Rahman A. A.**
The chemical environment in cements
Mat. Res. Soc. Symp. Proc. Vol. 44 (1985) p. 849

[7] **Longuet P.**
La protection des armatures dans le béton armé élaboré avec des ciments de laitier
Silicates Industriels 41(7/8) (1976) p. 321

[8] **Longuet P. , Burglen L. , Zelver A.**
La phase liquide du ciment hydraté
Revue des matériaux de constuction et de traveaux publics
676 (1973) p. 35

[9] **Flint E. P. , Wells L. S.**
Study of the system CaO–SiO_2–H_2O at 30°C and of the reaction of water on the anhydrous calcium silicates
J. Research NBS 12 (1934) p. 751

[10] **Fujii K. , Kondo W.**
Heterogeneous equilibrium of calcium silicate hydrate in water at 30°C.
J. Chem. Soc. Dalton Trans. 2 (1981) p. 645

[11] **Greenberg S. A. , Chang T. N.**
Investigation of the hydrated calcium silicates II. Solubility relationships in the calcium oxide - silica - water system at 25°C.
J. Phys. Chem. 69 (1965) p. 1151

[12] **Kalousek G. L.**
Application of differential thermal analysis in a study of the system lime–silica–water.
Proc. 3rd Int. Symp. on Chemistry of Cements, London (1952) p. 296

[13] **Roller P. S. , Ervin Jr. G.**
The system calcium oxide–silica–water at 30°C. The association of silicate ion in dilute alkaline solution.
J. Am. Chem. Soc. 62 (1940) p. 461

[14] **Taylor H. F. W.**
Hydrated calciumsilicates, part I. Compound formation at ordinary temperatures.
J. Chem. Soc. London 276 (1950) p. 3682

[15] **Berner U. R.**
Modelling the incongruent dissolution of hydrated cement minerals
Radiochimica Acta 44/45 (1988) p.387

[16] **Locher F. W.**
Stöchiometrie der Hydratation von Tricalciumsilicat.
Zement–Kalk–Gips 20(9) (1967) p. 402

[17] **Laske D. , Hübner W. , Künzle M. , Fischer P.**
Anwendungsbereite Zementrezepturen zur Verfestigung schwach- und mittelaktiver Abfälle aus Kernkraftwerken.
Nagra (National Cooperative for the Storage of Radioactive Waste)
Technischer Bericht NTB 84-09 (Baden, Switzerland, 1984)

[18] **Ludwig U. , Schwiete H. E.**
Untersuchungen an Deutschen Trassen
Mitteilungen aus dem Institut für Gesteinshüttenkunde der Rhein - Westf. Technischen Hochschule Aachen, presented at the Colloque "Puzzolanicité de l'Association belge pour favoriser l'étude des Verres et des Composés silicaux (Bruxelles, octobre 1962)

[19] **Scholtis A.**
OBS–1: Hydrogeochemische Untersuchungen am potentiellen Standort Oberbauenstock
Nagra (National Cooperative for the Storage of Radioactive Waste)
Interner Bericht NIB 88-45 (Baden, Switzerland, 1988)

[20] **Berner U. , Jacobsen J. , McKinley I. G.**
The near–field chemistry of a Swiss L/ILW repository
Proceedings of an NEA workshop on near–field Assessment of repositories for low and medium level radioactive waste, held in Baden, Switzerland, November 1987, OECD Paris 1988 p.197

[21] **Andersson K.**
Transport of radionuclides in water/mineral systems
Chalmers University of Technology, Goeteborg, Thesis 1983

[22] **Eikenberg J. , Laske D. , Berner U.**
Speziationsberechnungen von Zement-/Wasseranalysen
PSI Interner Bericht TM-41-89-08 (Würenlingen 1989)

[23] **Wanner H.**
Modelling interaction of deep groundwaters with bentonite and radionuclide speciation
EIR–Bericht Nr. 589 (Würenlingen 1986) and
Nucl. Technol. 79 (1987) p. 338

[24] **Sedimentstudie - Zwischenbericht 1988**
Möglichkeiten zur Endlagerung langlebiger radioaktiver Abfälle in den Sedimenten der Schweiz (Textband)
Nagra (National Cooperative for the Storage of Radioactive Waste)
Technischer Bericht NTB 88-25 (Baden, Switzerland, 1988)

[25] **Glasser F. P. et al.**
Medium active waste form characterization:
The performance of cement–based systems
in: Third Radioactive Waste Management Research Programme
University of Aberdeen, Old Aberdeen, Scotland
Progress Report of the CEC Contract F1 1W 0025UK(H) for the period Jan. 1987 – June 1987

[26] **Macphee D.**
University of Aberdeen, Old Aberdeen, Scotland
pers. communicaton 1988

[27] **Projekt Gewähr 1985**
Radioaktive Abfälle: Eigenschaften und Zuteilung auf die Endlager–Typen
Nagra (National Cooperative for the Storage of Radioactive Waste)
Gewähr–Bericht NGB 85-02 (Baden, Switzerland, 1985)

[28] **Bruno J. , Casas I. , Lagerman B. , Munoz M.**
The determination of the solubility of amorphous $UO_{2\ (s)}$ and the mononuclear hydrolysis constants of uranium(IV) at 25 °C.
Mat. Res. Soc. Symp. Proc. Vol. 84 (1987) p. 153

[29] **Atkinson A. , Hearne J. A. , Knights C. F.**
Aqueous chemistry and thermodynamic modelling of $CaO–SiO_2–H_2O$–gels
AERE R 12548 (Harwell Laboratory, UK, 1987)

[30] **Atkinson A. , Everitt N. M. , Guppy R.**
Evolution of pH in a radwaste repository: Experimental simulation of cement leaching
AERE R 12594 (Harwell Laboratory, UK, 1987)

[31] **Bradbury M. , Berner U.**
Proposals for the investigation of the sorption and transport properties of artificially "aged" cement
PSI Internal Report TM-41-88-01 (Würenlingen 1988)

[32] **Haworth A. , Sharland S. M. , Tweed C. J.**
Modelling of the degradation of cement in a nuclear waste repository
Mat. Res. Soc. Symp. Proc. Vol. 127 (1989) p. 447

[33] **Yeh G. T. , Tripathi V. S.**
A critical evaluation of recent developments in hydrogeochemical transport models of reactive multichemical components
Water Recources Research, Vol. 25/1 (1989) p.93

[34] **Haworth A. , Sharland S. M. , Tasker P. W. , Tweed C. J.**
A guide to the coupled chemical equilibria and migration code CHEQMATE
Nirex Report NSS/R113, HL88/1255 (Harwell Laboratory, UK, 1988)

[35] **Pourbaix M.**
Atlas of electrochemical equilibria in aqueous solutions
Ed. National Association of Corrosion Engineers, Houston, Texas (1974)

[36] **Baes C. F. Jr. , Mesmer R. E.**
The hydrolysis of cations
Ed. John Wiley & Sons, Inc. , New York (1976)

[37] **Grauer R.**
Zur Koordinationschemie der Huminstoffe
PSI-Bericht Nr. 24 (Würenlingen und Villigen, 1989)

[38] **Barrow G. M.**
Physikalische Chemie; Teil III: Mischphasenthermodynamik, Elektrochemie, Reaktionskinetik
Bohmann–Verlag, Heidelberg (1972) p. 109, ISBN 3 528 13548 4

[39] **Schweingruber M.**
Prinzipien der Speziationsrechnung – Grundlagen zur Einführung des Speziationsprogrammes MINEQL.
EIR Technische Mitteilung TM-45-80-21 (Würenlingen, 1980)

Schweingruber M.
Löslichkeits- und Speziationsberechnungen für U, Pu, Np und Th in natürlichen Gewässern – Theorie, thermodynamische Dateien und erste Anwendungen.
EIR–Bericht Nr. 449 (Würenlingen, 1981)

Schweingruber M.
User's guide for extended MINEQL (EIR version) – standard subroutine/data library package.

EIR Internal Report, TM-45-82-38 (Würenlingen, 1982)

Schweingruber M.
Revision 1 of: User's guide for extended MINEQL (EIR version) standard subroutine/data library package.
EIR Internal Report, AN-45-84-39 (Würenlingen, 1984)

[40] **Westall J. C. , Zachary J. L. , Morel F. M. M.**
MINEQL – A computer program for the calculation of chemical equilibrium compositions of aqueous systems.
MIT Technical Note No. 19 (1976)

[41] **Parkhurst D. L. , Thorstenson D. C. , Plummer L. N.**
PHREEQE – A computer program for geochemical calculations.
U.S.Geological Survey, Water Resources Division, Report PB81 167801 (1980)

[42] **NEA, OECD Nuclear Energy Agency, Paris, France**
NEA thermochemical data base, selected data set as of 4. July 1986.

[43] **Baeyens B. , Berner U. R.**
Procedure for defining selected reference waters for Untere Süsswasser Molasse (USM) and Opalinus Ton (OPA) sediments
PSI Internal Report TM-41-89-11 (Würenlingen 1989)

Appendix

A Basic thermodynamic considerations and assumptions; Outline of the procedure to extract model equations from experimental data.

A.1 Basic thermodynamic considerations

At constant pressure and constant temperature the equilibrium distribution of a component between the solid state and the dissolved state is described by:

$$\mu_0^{(s)} + RT \cdot \ln a^{(s)} = \mu_0^{(l)} + RT \cdot \ln a^{(l)}, \tag{5}$$

where R is the gas constant, T the absolute temperature, $a^{(s,l)}$ the activity of the component in the solid/dissolved state and the $\mu_0^{(s,l)}$ are the chemical potentials of 1 mole of the component in the solid state and in the dissolved state, respectively.

For a pure solid the activity $a^{(s)}$ in the solid is 1 by definition and, therefore, the activity of the component in the solution is constant:

$$\ln a^{(l)} = \frac{\mu_0^{(s)} - \mu_0^{(l)}}{RT} = \ln K_{so}. \tag{6}$$

K_{so} is called the "solubility product" of the solid. The model presented in section 3 assumes a nonideal mixture of two components which comprise the CSH–phase. In this case the activities of the components in the solid state differ from unity, but each component still is in equilibrium with the solution according to equation 5.

The Gibbs–Duhem equation for non-ideal mixtures [38] gives a relation between the solid state activities of the components in the non-ideal mixture:

$$d \ln a_1^{(s)} = -\frac{X_2}{X_1} \cdot d \ln a_2^{(s)}, \tag{7}$$

where X_1 and X_2 are the mole fractions of component 1 and 2, respectively. Integrating equation 7 gives:

$$\ln a_1^{(s)} = -\frac{X_2}{X_1} \cdot \ln a_2^{(s)} + C. \tag{8}$$

The integration constant C in equation 8 is a constant only for the particular mixture characterised by X_2/X_1. Concerning the CSH–phase, the integration constant C is a function of the C/S ratio. The following equations show, how C as a function of C/S can be derived from solubility data. For 1 mole of the mixture the free enthalpy of formation before mixing is given by:

$$G_{before} = X_1 \cdot \mu_{0,1}^{(s)} + X_2 \cdot \mu_{0,2}^{(s)}, \tag{9}$$

and the free enthalpy of formation after mixing by

$$G_{after} = X_1 \cdot \mu_{0,1}^{(s)} + X_1 \cdot RT \cdot \ln a_1^{(s)} + X_2 \cdot \mu_{0,2}^{(s)} + X_2 \cdot RT \cdot \ln a_2^{(s)}. \tag{10}$$

The free enthalpy of mixing is then given by:

$$\begin{aligned} \triangle G_{mix} &= G_{after} - G_{before} \\ &= RT \cdot \left[X_1 \cdot \ln a_1^{(s)} + X_2 \cdot \ln a_2^{(s)} \right]. \end{aligned} \tag{11}$$

Therefore, (equation 11 and 8) the integration constant C is given by

$$C = \frac{\triangle G_{mix}}{RT \cdot X_1}. \tag{12}$$

Unfortunately $\triangle G_{mix}$ for the CSH–phase (comprised by the model components given in section 3) is not known. Therefore we turn back to equation 8. If the solubility products of the pure components are known we can substitute the $\ln a_i^{(s)}$ by using equation 5 and 6:

$$\ln a_i^{(s)} = -\ln K_{so}^i + \ln a_i^{(l)} \qquad (i = 1,2). \tag{13}$$

Equation 13 says, that if a "well" known component is a part of a non-ideal mixture, its solid state activity can be derived from the known solubility product of the pure component and from the (measured) activity in the dissolved state.
By substituting $X_2 = 1 - X_1$ the integration constant C is given by

$$C = -\ln K_{so}^1 + \ln a_1^{(l)} + \frac{1 - X_1}{X_1} \cdot \left[-\ln K_{so}^2 + \ln a_2^{(l)} \right]. \tag{14}$$

And converting equation 14 from *ln* to *log* gives

$$C' = \log K_{so}^{2} - \log K_{so}^{1} + \log a_{1}^{(l)} - \log a_{2}^{(l)} + \frac{1}{X_1} \cdot \left[\log a_{2}^{(l)} - \log K_{so}^{2}\right]. \qquad (15)$$

In principle values of C′ as a function of the C/S ratio (or as a function of X_1) can be obtained from the experimental data. For region I and II the integration constant C′ is plotted in Figure 18 and 19 as a function of the C/S ratio. Neither from Figure 18 nor from Figure 19 a clear dependency of C′ on the C/S ratio can be concluded. Though Figure 18 indicates a linear dependency, a correlation factor r^2 of only 0.34 was found, indicating no true correlation.
It is therefore assumed that C′ is constant. This assumption is made for region I and also for region II.

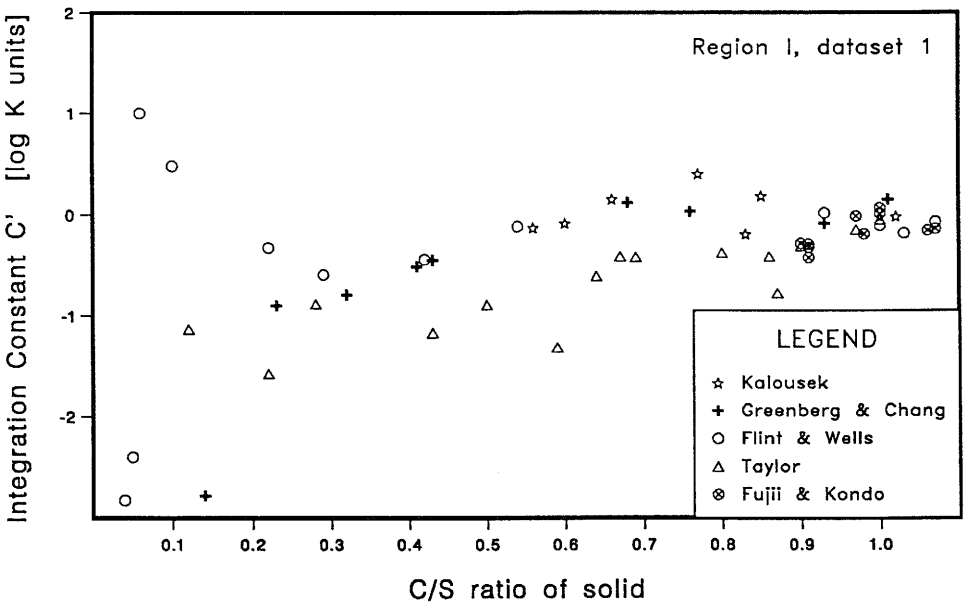

Figure 18: Integration constant C′ (cf. equation 15) vs. C/S ratio of CSH–phase (region I; dataset 1 from Table 2; T = 25°C).

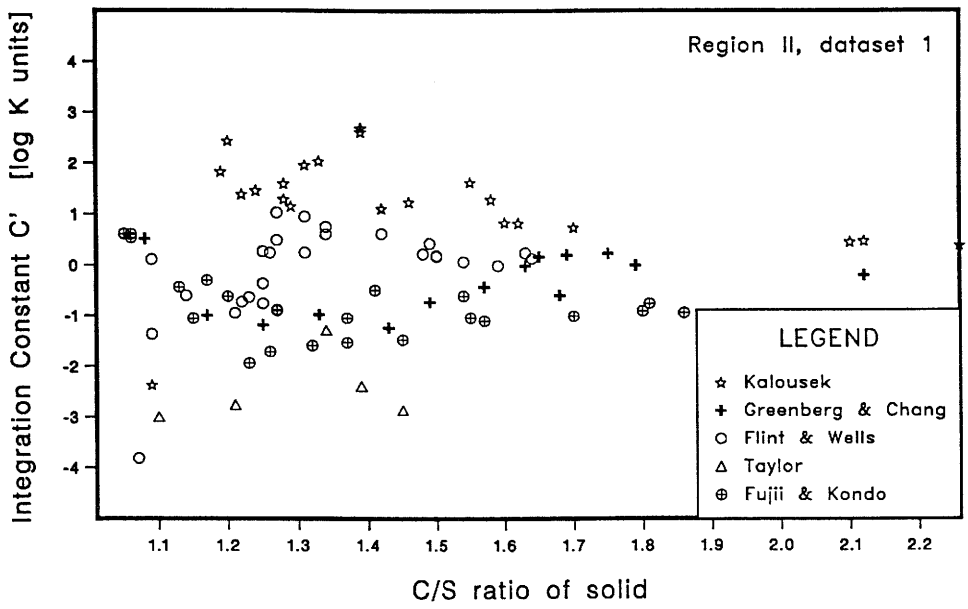

Figure 19: Integration constant C′ (cf. equation 15) vs. C/S ratio of CSH–phase (region II; dataset 1 from Table 2) T = 25°C.

By substituting equation 13 into equation 8 and converting $\log_e$ to $\log_{10}$ we obtain:

$$-\log K^1_{so} + \log a_1^{(l)} = -\frac{X_2}{X_1} \cdot \left[-\log K^2_{so} + \log a_2^{(l)}\right] + C'. \qquad (16)$$

It is important to note, that the $\log K^i_{so}$'s are the (normally known) solubility products of the pure components. The terms $a_i^{(l)}$ describe the solubility products of the model components at a given composition of the mixture. For this reason they are called "apparent solubility products" ($\hat{K}^i_{so}$).
These "apparent solubility products" depend on the composition of the mixture. For a given composition (C/S) they may be expressed in terms of equation 13:

$$\begin{aligned} \log a_i^{(l)}(C/S) &= \log a_i^{(s)}(C/S) + \log K^i_{so} \\ &= \log \hat{K}^i_{so}(C/S). \end{aligned} \qquad (17)$$

Using equations 16 and 17 the apparent solubility products of the two model components are related by

$$\log \hat{K}^1_{so} = P - \frac{1 - X_1}{X_1} \cdot \left[\log \hat{K}^2_{so} - Q\right], \tag{18}$$

with $P = C' + \log K^1_{so}$ and $Q = \log K^2_{so}$.
It is worthwhile to note, that equation 18 does not say how $\log \hat{K}^2_{so}$ depends on the composition of the mixture. This dependency has to be extracted from the data. On the other hand, if $\hat{K}^2_{so}$ as a function of the composition is known, equation 18 says, how $\hat{K}^1_{so}$ depends on $\hat{K}^2_{so}$ and on the composition of the mixture.

A.2 Extracting model equations from experimental data; outline of procedure

A.2.1 General

Analysis of equilibrium studies in the system $CaO–SiO_2–H_2O$ given by several authors [9,10, 11,12,13,14] has been performed using the speciation code MINEQL [39,40]. All data used in the present study are compiled in appendix B.
The composition (speciation) of each equilibrium system was calculated from total calcium and total silicon in solution, by assuming that the following set of dissolved species is present at equilibrium:

- Ca^{2+}
- $CaOH^+$
- $H_2SiO_4^{2-}$
- $H_3SiO_4^-$
- $H_4SiO_4^0$
- H^+
- OH^-

Due to some uncertainty concerning the thermodynamic properties of the silicate species $H_2SiO_4^{2-}$, $H_3SiO_4^-$ and $H_4SiO_4^0$ the calculations have been performed twice, using two slightly different basic datasets (dataset 1 and dataset 2; cf. Table 2 and [39,41,42]).
Polymeric silicate species are not considered within this study. The result from a speciation calculation is a set of activities of the species present (cf. above list) in the equilibrium solution. From these values the activities of the model solids in the dissolved state (the $a_i^{(1)}$'s, cf. equation 5) can be calculated.

Example:

$$\log\left\{Ca(OH)_2^0\right\} = \log\left\{Ca^{2+}\right\} + 2 \cdot \log\{OH^-\}, \tag{19}$$

where { } denotes the activity in the solution.

The apparent solubility product (the particular solubility at a given composition of the mixture) of a model solid is then calculated (equation 17) by:

$$\begin{aligned} \log \hat{K}_{so}^{Ca(OH)_2} &= \log\left\{Ca(OH)_2^0\right\}_{\text{dissolved}} \\ &= \log\left\{Ca^{2+}\right\} + 2 \cdot \log\{OH^-\}. \end{aligned} \tag{20}$$

A.2.2 Model equations for region II

The model solids associated with this C/S region are assumed to be $Ca(OH)_{2\ (s)}$ and $CaH_2SiO_{4\ (s)}$ (cf. Figure 3). According to equation 18 the apparent solubility products of the model solids are related by

$$\log \hat{K}_{so}^{Ca(OH)_2}(C/S) = P - \frac{1}{C/S - 1} \cdot \left[\log \hat{K}_{so}^{CaH_2SiO_4}(C/S) - Q\right], \tag{21}$$

where $X_{Ca(OH)_2}$ has been replaced by $\frac{C/S-1}{C/S}$ and $X_{CaH_2SiO_4}$ by $\frac{1}{C/S}$.

Plots of the calculated values of $\log \hat{K}_{so}^{Ca(OH)_2}$ and of $\log \hat{K}_{so}^{CaH_2SiO_4}$ vs. C/S ratio are given in Figure 20 and 21, respectively. $\log \hat{K}_{so}^{CaH_2SiO_4}$ was calculated using

$$\log \hat{K}_{so}^{CaH_2SiO_4} = \log\left\{Ca^{2+}\right\} + \log\left\{H_2SiO_4^{2-}\right\}$$

and $\log \hat{K}_{so}^{Ca(OH)_2}$ was calculated according to equation 20. From Figure 21 it is obvious that within region II no clear relationship $\log \hat{K}_{so}^{CaH_2SiO_4}$ vs. C/S is extractable. It is therefore assumed that $\log \hat{K}_{so}^{CaH_2SiO_4}$ has a <u>constant</u> value within region II. The actual value of $\log \hat{K}_{so}^{CaH_2SiO_4}$ can be extracted from Figure 22, which is an expanded section of Figure 21. Within the range $0.9 \leq C/S \leq 1.1$ $\log \hat{K}_{so}^{CaH_2SiO_4}$ is quite constant and an average of

$$\log \hat{K}_{so}^{CaH_2SiO_4} = -8.16 \pm 0.1$$

from 25 particular values was calculated using the basic dataset 1 (cf. Table 2). The value of $\log \hat{K}_{so}^{CaH_2SiO_4}$ is very sensitive to the basic thermodynamic data used for the speciation of

the silicate species. If dataset 2 is used instead of dataset 1, $\log \hat{K}_{so}^{CaH_2SiO_4}$ is shifted to -7.12. Greenberg [11] also used CaH_2SiO_4 as a model solid in order to model his experimental data (Greenberg's data are included in Figure 22). He reported a value of -7.0 ± 0.1 for $\log \hat{K}_{so}^{CaH_2SiO_4}$, using basic thermodynamic data for the silicate species similar to those given in dataset 2.

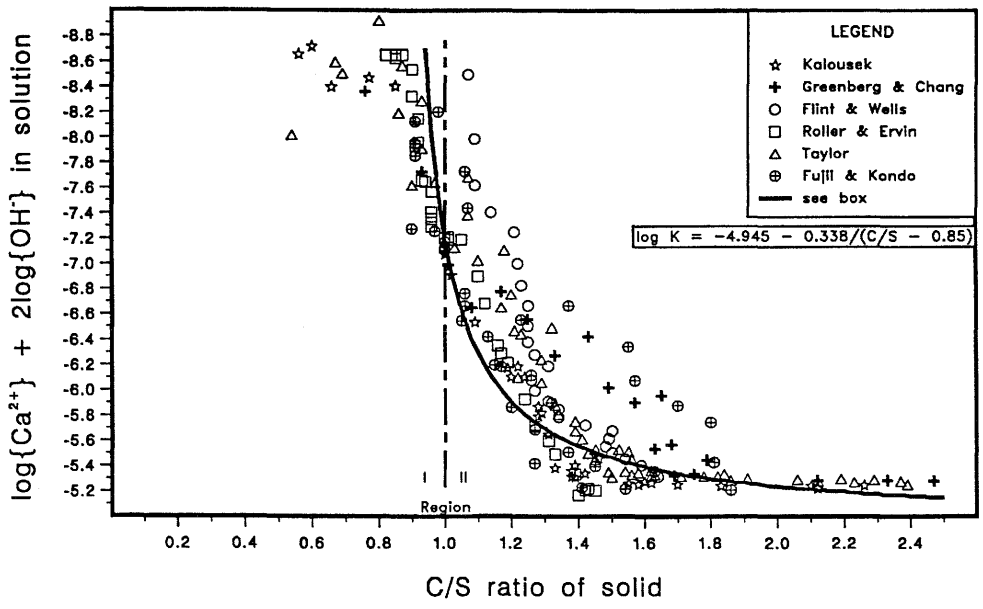

Figure 20: Apparent solubility product of $Ca(OH)_2$ vs. C/S ratio of solid (T = 25 °C).

Using the assumption that $\log \hat{K}_{so}^{CaH_2SiO_4}$ is constant, equation 21 is reduced to give

$$\log \hat{K}_{so}^{Ca(OH)_2}(C/S) \quad = \quad P - \frac{1}{C/S - 1} \cdot Q', \tag{22}$$

where P and Q′ are constants.
The analytical form of equation 22 implies an asymptotic behaviour at $C/S = 1$, which is a consequence of the composition of CaH_2SiO_4. From Figure 20 it can be seen that the asymptote in fact lies at $C/S \sim 0.85$. This means that the original assumption of CaH_2SiO_4 being a model solid may not be quite correct. A tobermorite-like model solid (i.e. $5CaO.6SiO_2.(7+z)H_2O$) which requires an asymptote at $C/S = 0.867$ would probably be more realistic, but such a model solid would also be much more complicated to handle. However, in order to fit the data given in Figure 20 an asymptote below $C/S = 1$ was chosen for two reasons:

1. To keep the basic model components as simple as possible,
2. To get a well defined value for $\log \hat{K}_{so}^{Ca(OH)_2}$ at C/S = 1. This is important in order to get a continuous transition from region II to region I.

The final results show that this choice does not affect the principal model conclusions. The fitting procedure was performed visually and a fit given by

$$\log \hat{K}_{so}^{Ca(OH)_2}(C/S) = -4.945 - \frac{0.338}{C/S - 0.85}, \tag{23}$$

was considered to be fair (cf. Figure 20, solid line).

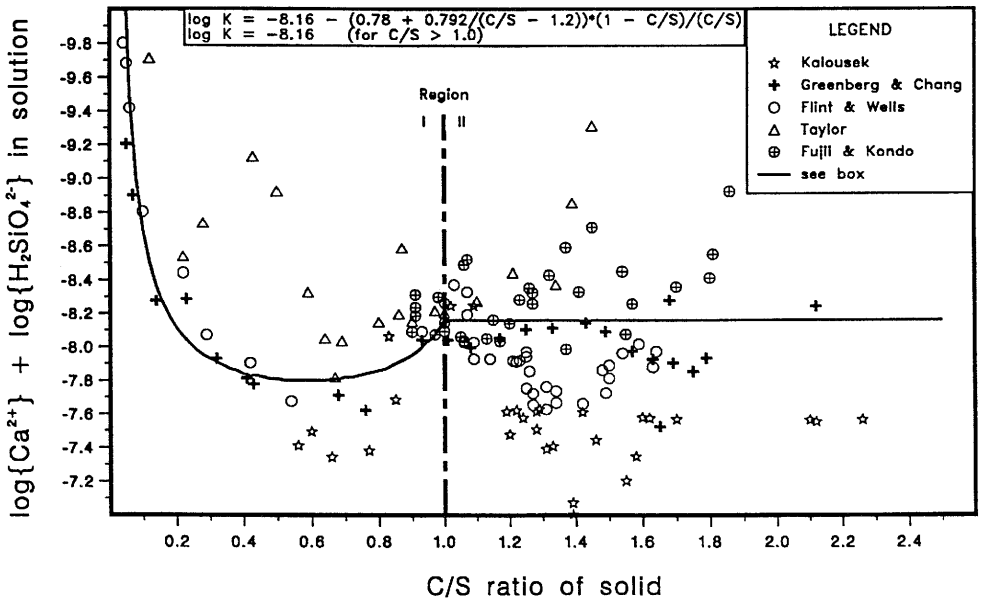

Figure 21: Apparent solubility product of CaH_2SiO_4 vs. C/S ratio of solid (T = 25 °C).

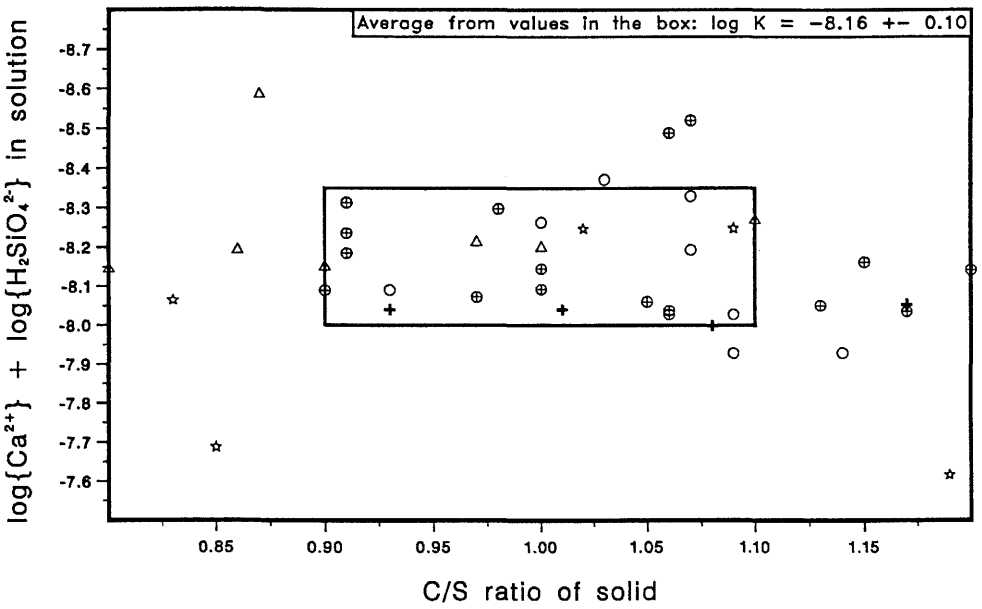

Figure 22: Apparent solubility product of CaH_2SiO_4 vs. C/S ratio of solid around C/S $\simeq$ 1. The figure is an expanded section of Figure 21)(T = 25 °C).

A.2.3 Model equations for region I

The model solids associated with this C/S region are assumed to be $SiO_{2(s)}$ and $CaH_2SiO_{4(s)}$ (cf. Figure 3). According to equation 18 the apparent solubility products of the model solids are related by

$$\log \hat{K}_{so}^{CaH_2SiO_4}(C/S) \quad = \quad P_1 - \frac{1 - C/S}{C/S} \cdot \left[\log \hat{K}_{so}^{SiO_2} - Q_1\right], \tag{24}$$

where X_{SiO_2} has been replaced by $1 - C/S$ and $X_{CaH_2SiO_4}$ by C/S.
A plot of $\log \hat{K}_{so}^{SiO_2}$(calculated as $\log \hat{K}_{so}^{SiO_2} = \log\left\{H_2SiO_4^{2-}\right\} + 2 \cdot \log\{H^+\}$; cf. equation 20) vs. the C/S ratio is given in Figure 23. In order to fit the data given in Figure 23 an analytical expression similar to the analytical expression used for $\log \hat{K}_{so}^{Ca(OH)_2}$ (cf. equation 23) was

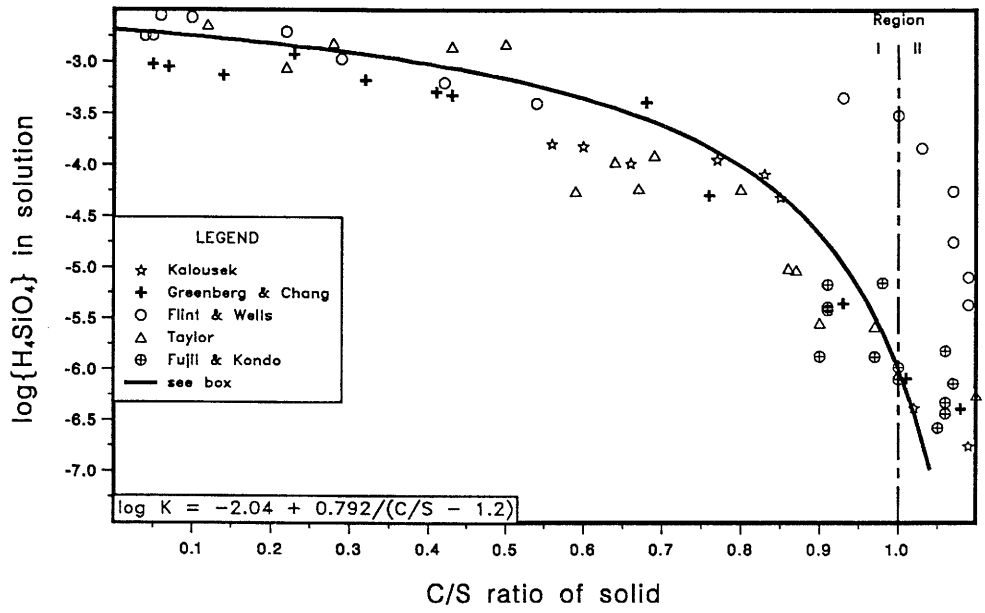

Figure 23: Apparent solubility product of SiO_2 vs. C/S ratio of solid (T = 25 °C).

chosen:

$$\log \hat{K}_{so}^{SiO_2}(C/S) \quad = \quad A + \frac{B}{C/S - \beta}. \tag{25}$$

This choice is based on the considerations that $\log \hat{K}_{so}^{SiO_2}$ has to reach asymptotically the true solubility of SiO_2 at low C/S ratios and an infinite negative value at $C/S \sim 1$.
Using equation 24 and equation 25 $\log \hat{K}_{so}^{CaH_2SiO_4}$ may be expressed as

$$\log \hat{K}_{so}^{CaH_2SiO_4} \quad = \quad P_1 - \frac{1 - C/S}{C/S} \cdot \left[A + \frac{B}{C/S - \beta} - Q_1\right]. \tag{26}$$

The equations 25 and 26 cannot directly be used to fit the "solubility" data given in Figure 22 and 23, respectively. These equations contain the adjustable parameters P_1, Q_1, A, B and β, which are related to each other by the following boundary conditions:

1. At $C/S = 0$, the value of $\log \hat{K}_{so}^{SiO_2}$ must correspond to the solubility of pure SiO_2.

2. In order to get a steady transition from region II to region I $\log \hat{K}_{so}^{CaH_2SiO_4}$ must be -8.16 at $C/S = 1$, as far as dataset 1 is concerned. The value is -7.12 using dataset 2.
3. At $C/S = 1$ the Ca^{2+} activities calculated from equation 23 and from equation 26 have to be equal.

From boundary condition 1 and from equation 25 it follows that (cf. also Table 3, page 10)

$$A - \frac{B}{\beta} = -2.70, \tag{27}$$

and from boundary condition 2 and from equation 26 it follows that

$$P_1 = -8.16 \qquad (\text{for} \beta \neq 1). \tag{28}$$

From boundary condition 3 and from equation 23 we calculate at $C/S = 1$

$$\log \hat{K}_{so}^{Ca(OH)_2} = \log \left\{Ca^{2+}\right\} + 2 \cdot \log \{OH^-\} = -7.198, \tag{29}$$

and from equations 26 and 28:

$$\log \hat{K}_{so}^{CaH_2SiO_4} = \log \left\{Ca^{2+}\right\} + \log \left\{H_2SiO_4^{2-}\right\} = -8.16. \tag{30}$$

At $C/S = 1$, $\log \left\{Ca^{2+}\right\}$ in 29 and 30 must be equal; therefore combining the two equations and replacing $\log \{OH^-\}$ by $(-14.00 - \log \{H^+\})$ gives

$$0 = 28.962 + \log \left\{H_2SiO_4^{2-}\right\} + 2 \cdot \log \{H^+\}. \tag{31}$$

According to the basic thermodynamic dataset 1 (cf. Table 2), $\log \left\{H_2SiO_4^{2-}\right\}$ and $\log \{H^+\}$ are related to $\log \left\{H_4SiO_4^0\right\}$ by

$$22.96 + \log \left\{H_2SiO_4^{2-}\right\} + 2 \cdot \log \{H^+\} = \log \left\{H_4SiO_4^0\right\}, \tag{32}$$

and, therefore, equation 31 can be written as

$$0 \quad = \quad 6.002 + \log\left\{H_4SiO_4^0\right\}. \tag{33}$$

Since $\log\left\{H_4SiO_4^0\right\}$ corresponds to the solubility of SiO_2, a second relationship between A, B and β is given by

$$A + \frac{B}{1-\beta} \quad = \quad -6.002. \tag{34}$$

By combining equation 27 and equation 34, A and B may be expressed in terms of β:

$$A \quad = \quad -2.70 - 3.302 \cdot (1-\beta) \tag{35}$$

$$B \quad = \quad -3.302 \cdot \beta \cdot (1-\beta). \tag{36}$$

The fit (which also was performed visually) for the apparent solubility of SiO_2 in region I (Figure 23) gave

$$\beta \quad \sim \quad 1.2$$

and therefore

$$\log \hat{K}_{so}^{SiO_2}(C/S) \quad = \quad -2.04 + \frac{0.792}{C/S - 1.2}. \tag{37}$$

The apparent solubility of CaH_2SiO_4 is then given by

$$\log \hat{K}_{so}^{CaH_2SiO_4}(C/S) \quad = \quad -8.16 - \frac{1-C/S}{C/S} \cdot \left[-2.04 + \frac{0.792}{C/S - 1.2} - Q_1\right]. \tag{38}$$

According to equation 18, Q_1 is the solubility of pure SiO_2 and should have a value of -2.70, but the shape of the curve given by equation 38 is very sensitive to Q_1. A value of

$$Q_1 \quad \sim \quad -2.82$$

has been selected to reproduce the solid line given in Figure 21.
Therefore, $\log \hat{K}_{so}^{CaH_2SiO_4}(C/S)$ in region I is given by

$$\log \hat{K}_{so}^{CaH_2SiO_4}(C/S) \quad = \quad -8.16 - \frac{1-C/S}{C/S} \cdot \left[0.78 + \frac{0.792}{C/S - 1.2}\right]. \tag{39}$$

A similar procedure was used to extract the model equations for the calculations performed with dataset 2, those results are compiled in Table 3, page 10.

A.3 Temperature dependency of the "apparent" solubility products

The experimental data considered in this study [9,10,11,12,13,14] (cf. Appendix B) have been evaluated at different temperatures (17°C, 25°C, 30°C) and an attempt has been made to convert the experimental data to 25°C. This section gives an outline of the corresponding converting procedure.
Within the geochemical speciation code MINEQL the temperature dependency of any log K - value is calculated using an approximated *van t'Hoff* equation [39]. With the assumptions that log K is not pressure-dependent and that the standard enthalpy of reaction ($\triangle H^0$) is constant within a small temperature range, log K(T) may be expressed as

$$\log K(T) = \log K(T_0) + \beta(T) \cdot \triangle H^0(T_0) \tag{40}$$

with

$$\begin{aligned} \triangle H^0 &= \text{standard enthalpy of reaction,} \\ \beta(T) &= \left(\frac{1}{T_0} - \frac{1}{T}\right) \Big/ R \cdot \ln 10, \\ R &= \text{Gas constant,} \\ T_0 &= 298.15 \quad K. \end{aligned}$$

Since the equilibrium constant for a given reaction is related to the *Gibbs* free energy by

$$\log K = C \cdot \triangle G_r^0 \tag{41}$$

with

$$C = -\frac{1}{R \cdot T \cdot \ln 10} \qquad (C = -0.1752 \quad \text{moles/kJ} \quad \text{at} \quad 25°C), \tag{42}$$

and $\triangle G_r^0$ of the reaction may be expressed as

$$\triangle G_r^0 = \triangle H_r^0 - T \cdot \triangle S_r^0 \tag{43}$$

with $\triangle S_r^0$ being the standard entropy of reaction, an apparent solubility product $\log \hat{K}_{so}^i$ as proposed in A.1 may be expressed as

$$\log \hat{K}_{so}^i = C \cdot \triangle \hat{G}_r^0 = \left[\triangle \hat{H}_r^0 - T \cdot \triangle \hat{S}_r^0\right]. \quad (44)$$

For a given model solid *i*, the difference between the true solubility and the apparent solubility is given by

$$\log K_{so}^i - \log \hat{K}_{so}^i = C \cdot \left[\triangle H_i^0 - \triangle \hat{H}_i^0 - T \cdot \left(\triangle S_i^0 - \triangle \hat{S}_i^0\right)\right]. \quad (45)$$

Due to the lack of data on $\triangle \hat{H}_i^0$ and $\triangle \hat{S}_i^0$ it is assumed that $\triangle S^0$ does not change with C/S and therefore

$$\triangle S_i^0 = \triangle \hat{S}_i^0 .$$

With this assumption $\triangle \hat{H}_i^0$ at $T = T_0$ can be calculated from

$$\triangle \hat{H}^0 = \frac{1}{C(T_0)} \cdot \left(\log \hat{K}_{so}^i - \log K_{so}^i\right) + \triangle H_i^0. \quad (46)$$

Combining equations 40 and 46 the temperature dependency of an apparent solubility product may be expressed as

$$\log \hat{K}_{so}^i(T) = \frac{T_0}{T} \cdot \log \hat{K}_{so}^i(T_0) - \left(\frac{T_0}{T} - 1\right) \cdot \log K_{so}^i(T_0) + \beta(T) \cdot \triangle H_i^0(T_0). \quad (47)$$

Equation 47 has been used to convert the experimental data to 25°C.
Instead of assuming a C/S–independent standard entropy of reaction ($\triangle S_i^0 = \triangle \hat{S}_i^0$), a C/S–independent standard enthalpy of reaction ($\triangle H_i^0 = \triangle \hat{H}_i^0$) could have been proposed. Equation 47 would then have the form

$$\log \hat{K}_{so}^i(T) = \log \hat{K}_{so}^i(T_0) + \beta(T) \cdot \triangle H_i^0(T_0). \quad (48)$$

However, within a temperature range of, say 15°C to 35°C the $\log \hat{K}_{so}^i(T)$–values from equation

47 and 48 do certainly not differ by more than ± 0.1 logK - units (based on the thermodynamic "constants" given in Table 2 and 3), and it is not expected that this would change the final model results remarkable.
In a strict sense the model equations derived in section A.2.2 and A.2.3 are only valid at 25°C, due to the boundary conditions given on page 54. If, in spite of this, equation 47 is used to model the solubility of CSH–phases at temperatures different from 25°C, it has to be noted, that these boundary conditions are not fulfilled anymore. The results may become inconsistent, especially near C/S = 1. As an indication, the temperature dependency of the model solid solubilities at C/S = 1, according to equation 47 is given in Table 9.

Table 9: Temperature dependency of model solid solubilities at C/S = 1 calculated with equation 47; values from dataset 1 (Table 2) have been considered.

T	$\log \hat{K}_{so}^{Ca(OH)_2}(T)$	$\log \hat{K}_{so}^{CaH_2SiO_4}(T)$	$\log \hat{K}_{so}^{SiO_2}(T)$
5°C	-7.12	-7.48	-6.47
10°C	-7.14	-7.66	-6.35
15°C	-7.16	-7.83	-6.23
20°C	-7.18	-8.00	-6.11
25°C	-7.20	-8.16	-6.00
30°C	-7.22	-8.32	-5.89
35°C	-7.24	-8.47	-5.79
40°C	-7.25	-8.61	-5.69
45°C	-7.27	-8.75	-5.59

B Compilation of literature data

The following tables give a compilation of all literature data used within the model calculations. In particular, for each equilibrium system the following parameters are given (if available):

Column 1	C/S ratio of the solid which is in equilibrium with the solution
Column 2	total Calcium concentration of equilibrium solution
Column 3	total Silica concentration of equilibrium solution
Column 4	pH of equilibrium solution
Column 5	Indicator which describes the process to reach equilibrium (D = dissolution process, P = precipitation process)

Table 10: Data from *Flint & Wells* [9], measured at 30°C.

C/S ratio	Ca_{tot} mmoles/litre	$SiO_{2\ tot}$ mmoles/litre	pH	Indicator
0.04	0.49	2.95	—	P
0.05	0.54	3.06	—	P
0.06	0.77	4.64	—	P
0.10	1.25	5.43	—	P
0.22	1.52	5.11	—	P
0.29	1.70	4.34	—	P
0.42	1.68	3.67	—	P
0.54	1.81	3.43	—	P
0.93	1.32	2.73	—	P
1.00	1.05	1.99	—	P
1.03	0.86	1.26	—	P
1.07	0.88	0.77	—	P
1.07	1.18	0.44	—	P
1.09	1.68	0.31	—	P
1.09	2.23	0.23	—	P
1.14	2.64	0.17	—	P
1.21	3.00	0.14	—	P
1.22	3.71	0.10	—	P
1.23	4.32	0.077	—	P
1.25	4.98	0.055	—	P
1.25	5.76	0.073	—	P
1.25	6.44	0.040	—	P

cont. Table 10 (Data from *Flint & Wells* [9])

C/S ratio	Ca_{tot} mmoles/litre	$SiO_{2\ tot}$ mmoles/litre	pH	Indicator
1.27	7.08	0.058	—	P
1.31	7.70	0.047	—	P
1.26	8.52	0.033	—	P
1.27	9.24	0.047	—	P
1.31	9.99	0.045	—	P
1.34	10.61	0.038	—	P
1.39	11.25	0.030	—	P
1.42	11.97	0.033	—	P
1.50	12.52	0.022	—	P
1.49	13.30	0.025	—	P
1.48	14.11	0.017	—	P
1.50	14.84	0.015	—	P
1.54	15.59	0.012	—	P
1.59	16.35	0.010	—	P
1.63	17.14	0.013	—	P
1.64	17.89	0.010	—	P
1.12	5.26	—	11.73	P
1.21	5.38	—	11.74	P
1.18	5.76	—	11.76	P
1.20	5.97	—	11.78	P
1.19	6.29	—	11.80	P
1.20	6.55	—	11.81	P
1.22	6.73	—	11.82	P
1.31	6.91	—	11.83	P
1.29	7.25	—	11.85	P
1.25	7.57	—	11.87	P
1.27	7.83	—	11.89	P
1.83	12.46	—	12.06	P
1.84	13.11	—	12.08	P
1.86	13.76	—	12.10	P
1.85	14.44	—	12.12	P

Table 11: Data from *Roller & Ervin Jr.* [13], measured at 30°C.

C/S ratio	Ca_{tot} mmoles/litre	$SiO_{2\ tot}$ mmoles/litre	pH	Indicator
0.87	0.90	—	—	D
0.85	0.90	—	—	D
0.82	0.90	—	—	D
0.85	0.92	—	—	D
0.90	0.99	—	—	D
0.90	1.18	—	—	D
0.92	1.37	—	—	D
0.92	1.60	—	—	D
0.91	1.64	—	—	P
0.93	2.07	—	—	D
0.94	2.09	—	—	D
0.96	2.24	—	—	D
0.96	2.57	—	—	D
0.96	2.69	—	—	D
0.96	2.84	—	—	D
1.01	3.05	—	—	D
1.00	3.07	—	—	P
1.05	3.10	—	—	P
1.01	3.11	—	—	P
1.05	3.11	—	—	D
1.10	4.02	—	—	D
1.12	4.89	—	—	P
1.16	6.60	—	—	P
1.17	6.99	—	—	D
1.19	7.49	—	—	P
1.24	9.81	—	—	D
1.27	12.08	—	—	P
1.31	13.53	—	—	P
1.33	14.98	—	—	P
1.39	17.51	—	—	P
1.43	19.60	—	—	P
1.42	19.90	—	—	P
1.45	19.96	—	—	P
1.40	20.67	—	—	P

cont. Table 11 (Data from *Roller & Ervin Jr.* [13])

C/S ratio	Ca_{tot} mmoles/litre	$SiO_{2\ tot}$ mmoles/litre	pH	Indicator
—	20.47	0.011	—	P
—	15.36	0.015	—	P
—	8.76	0.024	—	P
—	6.24	0.034	—	P
—	4.54	0.051	—	P
—	3.52	0.078	—	P
—	3.41	0.082	—	P
—	3.16	0.092	—	P
—	2.92	0.108	—	P
—	2.84	0.112	—	P
—	2.81	0.107	—	P
—	2.70	0.114	—	P
—	2.69	0.119	—	P
—	2.55	0.140	—	P
—	1.83	0.215	—	P
—	1.64	0.267	—	P
—	1.52	0.293	—	P
—	1.18	0.442	—	P
—	1.01	0.666	—	P
—	0.99	0.690	—	P

Table 12: Data from *Taylor* [14], measured at 17°C.

C/S ratio	Ca_{tot} mmoles/litre	$SiO_{2\ tot}$ mmoles/litre	pH	Indicator
0.12	0.81	3.43	—	P
0.43	1.11	3.27	—	P
0.50	1.34	3.79	—	P
0.22	1.55	3.60	—	P
0.28	1.57	4.25	—	P
1.39	13.04	0.004	—	P
1.86	20.64	—	—	P
1.18	3.75	—	—	D
1.52	16.18	—	—	D
1.56	17.46	—	—	D
1.82	20.06	—	—	D
1.91	20.37	—	—	D
0.54	1.71	—	—	D
0.59	1.13	1.12	—	D
0.69	1.14	—	—	D
0.80	1.31	1.32	—	D
0.64	1.46	1.94	—	D
0.69	1.50	2.10	—	D
0.86	1.65	0.47	—	D
0.67	1.73	1.74	—	D
0.87	1.20	0.332	—	D
0.93	1.36	—	—	D
0.93	1.87	—	—	D
0.97	2.43	0.209	—	D
0.90	2.49	0.233	—	D
1.00	3.60	0.111	—	D
1.10	4.06	0.078	—	D
1.34	12.36	0.013	—	D
1.45	17.53	0.001	—	D
1.07	2.27	—	—	D
1.07	2.94	—	—	D
1.03	3.69	—	—	D

cont. Table 12 (Data from *Taylor* [14])

C/S ratio	Ca_{tot} mmoles/litre	$SiO_{2\ tot}$ mmoles/litre	pH	Indicator
1.20	5.14	—	—	D
1.17	5.63	—	—	D
1.29	8.21	—	—	D
1.22	9.36	—	—	D
1.23	6.80	—	—	D
1.29	9.73	—	—	D
1.33	11.55	—	—	D
1.39	14.05	—	—	D
1.41	14.92	—	—	D
1.45	16.21	—	—	D
1.43	16.69	—	—	D
1.62	19.06	—	—	D
1.54	19.24	—	—	D
1.49	19.35	—	—	D
1.56	19.75	—	—	D
1.63	19.75	—	—	D
1.50	20.15	—	—	D
1.58	19.38	—	—	D
1.71	19.98	—	—	D
1.32	6.51	—	—	D
1.21	6.66	0.025	—	D
1.55	16.47	—	—	D
1.84	19.70	—	—	D
1.62	19.88	—	—	D
1.78	19.98	—	—	D
2.19	20.42	—	—	D
2.06	20.51	—	—	D
2.29	20.62	—	—	D
2.12	20.72	—	—	D
2.37	20.83	—	—	D
2.23	20.97	—	—	D
2.39	21.35	—	—	D

Table 13: Data from *Kalousek* [12], measured at 25°C.

C/S ratio	Ca_{tot} mmoles/litre	$SiO_{2\ tot}$ mmoles/litre	pH	Indicator
0.56	2.16	3.10	—	P
0.60	2.00	2.83	—	P
0.66	2.02	2.66	—	P
0.77	2.14	2.68	—	P
0.83	1.19	1.33	—	P
0.85	1.66	1.36	—	P
1.00	3.58	—	—	P
1.02	4.17	0.05	—	P
1.09	5.83	0.03	—	P
1.19	8.15	0.08	—	P
1.20	8.72	0.10	—	P
1.22	8.04	0.08	—	P
1.24	8.68	0.04	—	P
1.28	11.66	0.05	—	P
1.29	11.36	0.05	—	P
1.28	10.84	0.07	—	P
1.31	13.41	0.07	—	P
1.46	16.12	0.05	—	P
1.42	18.12	0.03	—	P
1.33	17.40	0.05	—	P
1.39	16.99	0.13	—	P
1.38	17.78	—	—	P
1.39	18.69	0.10	—	P
1.38	18.55	—	—	P
1.58	19.78	0.05	—	P
1.55	19.67	0.07	—	P
1.62	19.54	0.03	—	P
1.60	19.33	0.03	—	P
1.70	19.79	0.03	—	P
2.12	20.44	0.03	—	P
1.83	19.99	—	—	P
2.10	19.99	0.03	—	P
2.26	19.94	0.03	—	P

Table 14: Data from *Greenberg & Chang* [11], measured at 25°C.

C/S ratio	Ca_{tot} mmoles/litre	$SiO_{2\ tot}$ mmoles/litre	pH	Indicator
0.05	0.74	2.31	9.32	P
0.07	0.93	2.60	9.16	P
0.14	1.47	3.40	9.65	P
0.23	1.68	4.33	9.75	P
0.76	1.75	1.47	10.48	P
0.32	1.90	4.07	9.80	P
0.41	1.95	3.90	9.98	P
0.43	1.97	3.87	10.02	P
0.68	2.00	3.77	10.26	P
0.93	2.13	0.25	11.40	P
1.01	3.90	0.09	11.77	P
1.17	4.71	0.065	11.90	P
1.08	5.28	0.062	11.92	P
1.25	5.72	0.043	11.95	P
1.43	6.45	0.033	12.10	P
1.33	7.42	0.029	12.10	P
1.49	9.42	0.022	12.14	P
1.57	10.50	0.025	12.16	P
1.63	15.00	0.018	12.25	P
1.79	16.40	0.016	12.33	P
1.69	18.50	0.015	12.40	P
1.65	10.0	0.075	12.40	D
1.68	14.5	0.008	12.46	D
1.75	18.3	0.017	12.50	D
2.12	19.2	0.007	12.45	D
2.33	19.2	—	12.60	D
2.47	19.3	—	12.46	D

Table 15: Data from *Fujii & Kondo* [10], measured at 30°C.

C/S ratio	Ca_{tot} mmoles/litre	$SiO_{2\ tot}$ mmoles/litre	pH	Indicator
0.91	1.48	0.237	—	D
1.00	3.37	0.068	—	D
1.37	4.98	0.053	—	D
1.55	6.67	0.028	—	D
1.57	8.54	0.013	—	D
1.70	10.31	0.008	—	D
1.80	11.71	0.006	—	P
1.81	15.97	0.003	—	P
1.86	19.85	0.001	—	P
0.98	1.39	0.230	—	D
1.06	1.98	0.075	—	D
1.07	2.52	0.046	—	D
1.23	5.50	0.023	—	D
1.26	8.22	0.011	—	P
1.32	10.10	0.007	—	P
1.37	14.73	0.003	—	P
1.45	16.84	0.002	—	P
0.91	1.67	0.155	—	D
0.90	2.92	0.098	—	D
1.05	5.55	0.038	—	D
1.15	7.63	0.019	—	D
1.20	10.46	0.013	—	P
1.27	12.39	0.008	—	P
1.27	16.12	0.005	—	P
1.41	19.49	0.004	—	P
1.54	19.68	0.003	—	P
0.91	1.82	0.180	—	P
0.97	2.97	0.099	—	P
1.00	3.19	0.084	—	P
1.06	4.57	0.055	—	P
1.06	4.99	0.047	—	P
1.13	6.20	0.033	—	P
1.17	7.72	0.025	—	P